

https://dspace.org/

Ligand design using the neutral oxygen donor to control metal ion size selectivity

Bhavan, Rekha

2015-01-08
http://hdl.handle.net/10539/16271

Downloaded from a DSpace repository. https://dspace.org/

open–chain analogues. However, the decrease in stability for large metal ions was sharper than for the smaller metal ions, which is in accord with large chelate rings causing destabilization of large metal ions.

These observations form an important feature in ligand design, namely, that five–membered chelate rings favour complexation of large metal ions whereas six–membered chelate rings favour the complexation of small metal ions. This effect is independent of the macrocyclic structure.

1.6 THE ROLE OF THE OXYGEN DONOR IN CONTROLLING COMPLEX STABILITY.

A large variety of ligands exist which contain almost exclusively neutral oxygen donor atoms, such as the crown ethers (2) and the nonactin and monensin (Fig. 1.6.1) family of antibiotics (65). These ligands show successful complex formation with large metal ions.

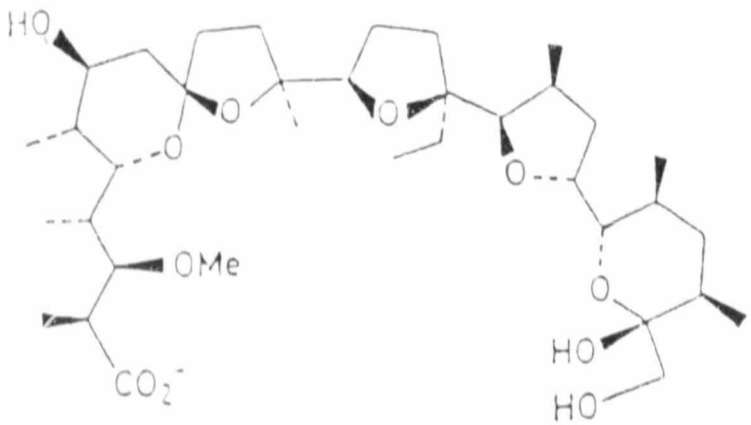

Fig. 1.6.1 Monensin–A antibiotic

Prior to Pedersen's discovery of the crown ethers (2), ligands bearing neutral oxygen donor atoms in the form of alcoholic or ethereal groups had been investigated but appeared to show no interesting complexing properties (52). The

recent interest in ligands bearing alcoholic or ethereal oxygens in side arms (53–56) such as the "Lariat Ethers" of Gokel et al. (53) have led to a considerable interest in the neutral oxygen donor.

An important idea in crown ether chemistry has been that of hole–size–selectivity, i.e. metal ions are most strongly complexed where there is a match between the size of the metal ion and the macrocyclic cavity. It has been shown by Gokel et al. (29,57,59) and Lichaux and Reisse (28) that cation selectivity in macrocycles, such as the crown ethers and lariat ethers, is not governed by the macrocyclic cavity but rather by the number of oxygen donors present.

A more extensive and systematic investigation on the effect of the oxygen donor on complex stability has been carried out by Hancock et al. (32,58,60–62,64). Their first investigation on this effect involved the study of complex formation with the ligands ethanolamine (61) and triethanolamine (60). These ligands are derived from ammonia by the addition of hydroxyethyl groups. The authors demonstrated (60) that small metal ions such as Cu^{2+}, Ni^{2+} and Zn^{2+} showed little change in complex stability whereas the larger metal ion, Pb^{2+}, showed a large increase in complex stability when hydroxyethyl groups are added to ammonia. It was observed that the increase in stability was size–related and would be found for large metal ions whether the added oxygen donor was alcoholic or ethereal, part of the macrocyclic ring or a pendent donor group. To examine this hypothesis, the stability of the complexes formed with various polyamine ligands was examined. This involved open–chain ligands containing oxygen donors (32,62,64), macrocycles containing oxygen donors (32) and macrocycles containing oxygen donors as pendent groups (58,62). Some of these ligands, where the progressive increase in the number of oxygen donors lead to an increase in the Pb^{2+} over Zn^{2+} selectivity, are shown in Fig. 1.6.2.

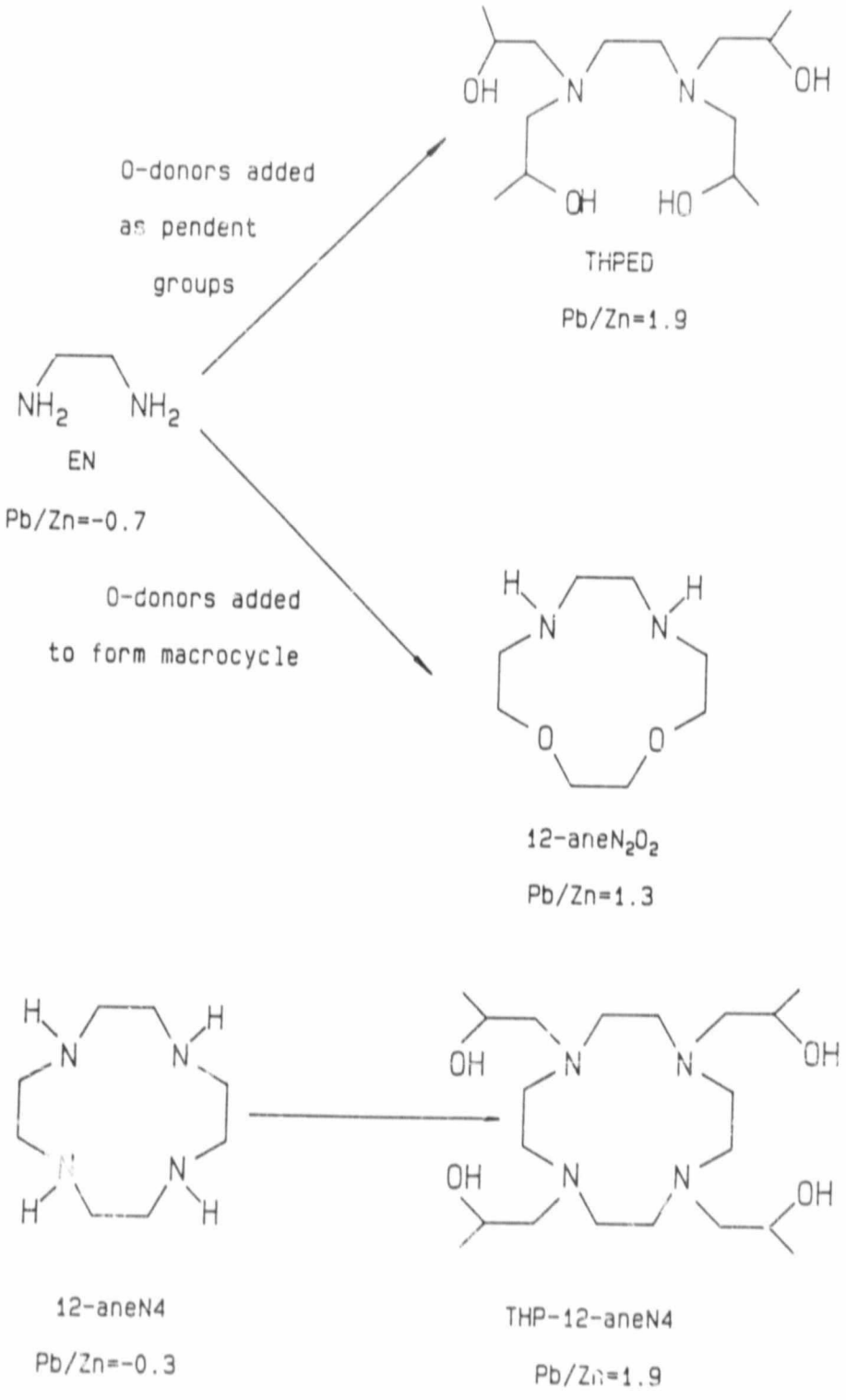

Fig. 1.6.2 Effect of addition of neutral oxygen donor groups to an existing ligand on the Pb^{2+}/Zn^{2+} selectivity. The Pb^{2+}/Zn^{2+} selectivity is log $K_1(Pb^{2+})$ minus log $K_1(Zn^{2+})$ for each ligand.

It was evident from these studies that addition of neutral oxygen donor groups increases the selectivity of the ligand for large relative to small metal ions. This increase was observed irrespective of whether the oxygen donor was part of a macrocyclic ring, an open chain or a pendent donor group. However, the size–selectivity produced was sharper for the macrocyclic ligands compared to the open–chain ligands.

The above authors have shown that the relationship between change in complex stability which accompanies addition of neutral oxygen donors, and the ionic radius of the metal ion is so close that a linear relationship is obtained for Δlog K plotted against ionic radius, r'. This is seen in Fig. 1.6.3 for Δlog K for EN going to THPED (open–circles) and for EN going to cryptand–2,2,2 (solid circles). The change in complex stability, Δlog K accompanying the changes in structure is seen to be a function of the size of the metal ion. The slope for the Δlog K versus r' relationship for cryptand–2,2,2 is much steeper than that for THPED, indicating that the presence of the macrocyclic ring leads to sharper metal ion size selectivity. As shown in Fig. 1.6.3, smaller metal ions show less favourable changes in complex stability than do larger metal ions when groups containing neutral oxygen donors are added to an existing ligand.

An automatic increase in complex stability is expected when groups bearing neutral oxygen donors are added to an existing ligand by virtue of the expected chelate effect (104). However, Hancock et al. (32) has shown that the contribution from the chelate effect would be nullified since the solvent water is a unidendate analogue for the alcoholic oxygen arm and is present in a 55.5M excess over any ligand dissolved in it. This cancels out the contribution of log 55.5, which is the entropy contribution to the chelate effect (105) in terms of Adamson's proposals (106), and thus no chelate effect results (32).

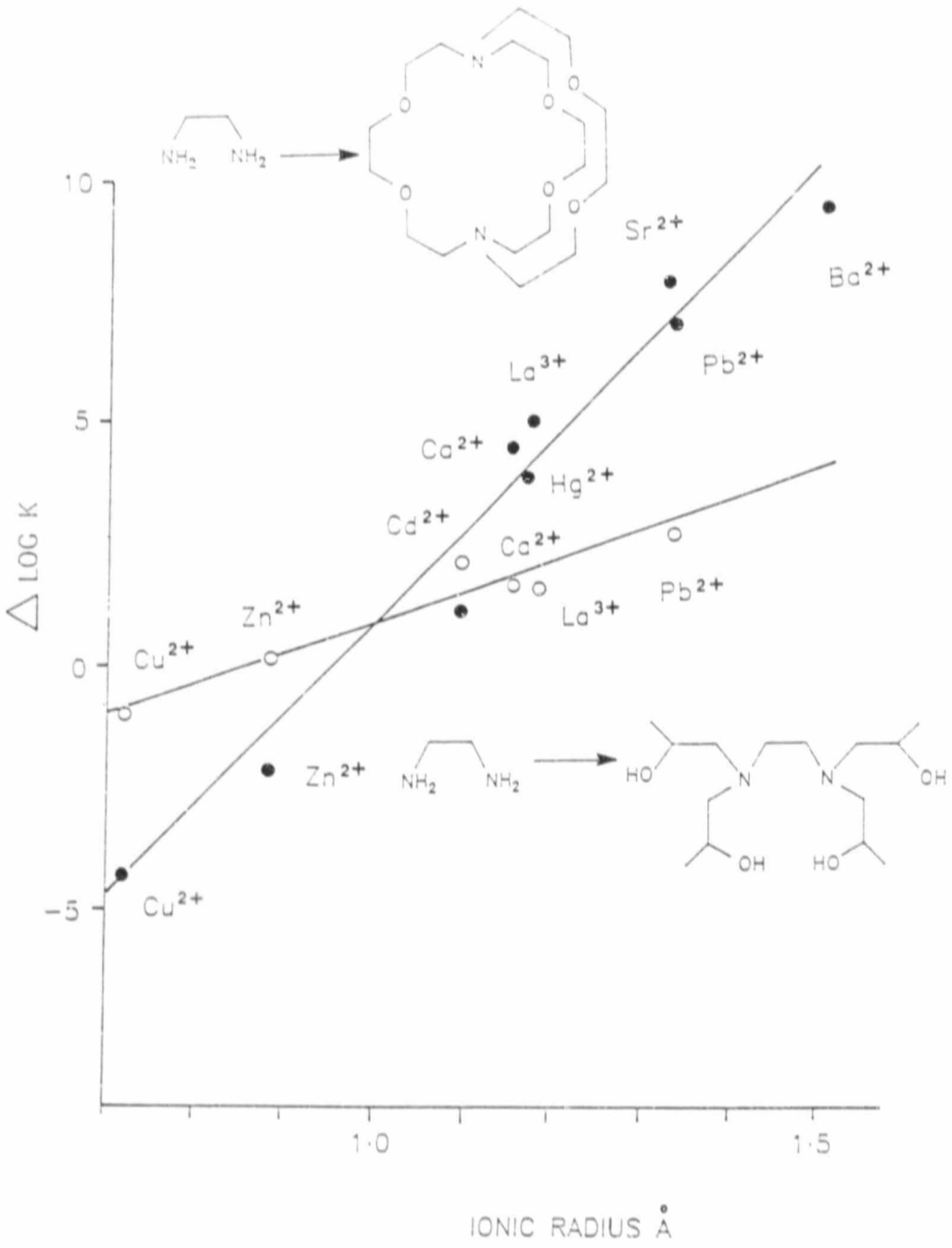

Fig. 1.6.3 Relationship between the change in complex stability, Δ log K, and the ionic radius for a variety of metal ions. The Δ log K values are for passing from EN to THPED and for EN going to cryptaind–2,2,2. Data from ref. 61 and 62.

The behaviour observed in Fig. 1.6.3 was explained in terms of the balance which exists between steric and inductive effects (60,62). Studies of gas phase basicities (14) indicate that the basicity of the neutral oxygen donor increases in the order $H_2O<ROH<R_2O$, where R = alkyl group. Addition of an ethereal or alcoholic group will thus produce favourable inductive effects due to the electron releasing properties of the alkyl group. In the case of EN going to THPED, four waters are changed to alcoholic oxygens and thus an increase in complex stability is observed for large metal ions (62). As the metal ion size decreases, the steric strain around the metal ion which is produced by the alkyl groups, outweighs the favourable inductive effects, leading to a nett destabilization of complex formation (62).

For small metal ions the steric crowding around the metal ion should lead to bond deformation and distortion of the bond angles around the metal ions. This is well illustrated for the small metal ion Ni^{2+} where the progressive addition of ethylene groups to Ni^{2+} complexes leads to an increase in the Ni–O bond length from 2.06Å to 2.15Å (Fig. 1.6.4)(64,73–75).

The origin of the Ni–O bond stretching is the Van de Waals repulsive interactions between the hydrogens on the ethylene bridges of the ligand which pulls the oxygen out (64). The bond stretching effect has been reproduced by molecular mechanics calculations, proving that it is a steric and not an inductive effect.

For large metal ions, even though the coordination number tends to increase, steric effects are outweighed by the inductive effects, and an increase in stability occurs.

The above observations have led to a second rule useful for ligand design: the addition of neutral oxygen donor groups to ligands increases the selectivity of the ligand for large relative to small metal ions. The main emphasis of this work is to investigate further the size–selectivity properties of the neutral oxygen donor. The

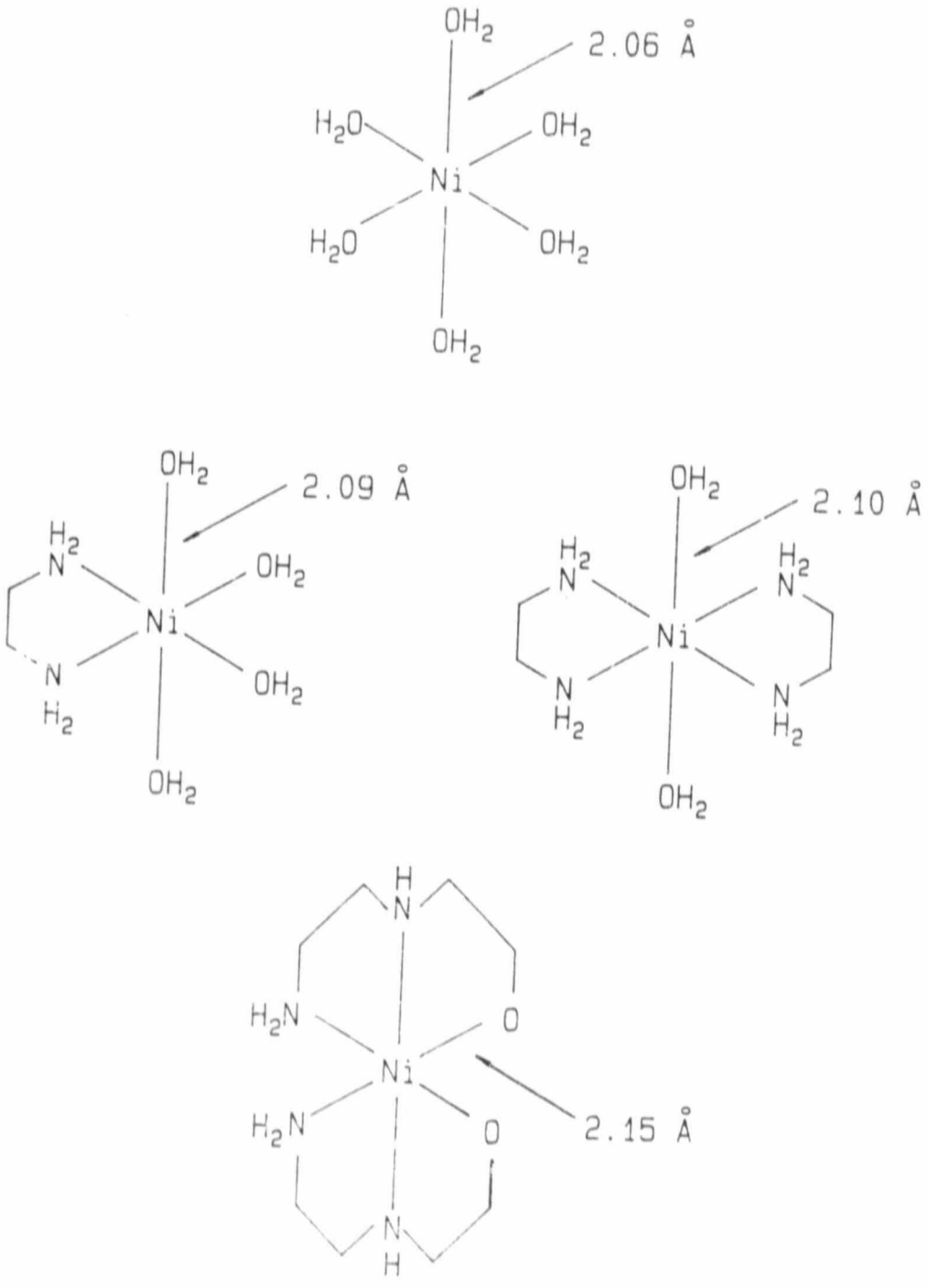

Fig. 1.6.4 The progressive increase in steric crowding around the small metal ion Ni^{2+}, leads to an increase in the Ni–O bond length.

ability to control metal ion selectivity is of interest in many areas, amongst which are reagents as imaging agents in medicine (6c) and for the treatment of metal intoxication in cases of metal poisoning (6a). The immediate interest in this work is in the development of ligands as therapeutic agents for the treatment of lead intoxication.

1.7 RIGID MACROCYCLIC LIGANDS

An important feature that has emerged from Section 1.4 is that the tetraazamacrocycles and the crown ethers are too flexible to display "hole–size–selectivity". In order to observe this match between the cavity size and metal ion size, it is necessary to make the macrocyclic ligands more rigid. In doing so, the metal ion will be forced to coordinate in the plane of the donor atoms.

This "hole–size–selectivity" relationship is observed for the relatively inflexible, three–dimensional cation binders devised by Lehn which are called the cryptands (63,76). A variety of other extremely rigid macrocycles have been designed and synthesized and include the spherands (77), cavitands (78), sepulchrates and the sarcophaginates (Fig. 1.7.1)(79). The cavity sizes of these macrocyclic ligands differ and so metal ions of sizes best suited for the cavity should complex more strongly with these ligands. The spherands complex strongly to Li^+ and Na^+ ions (80), the cavity of the sepulchrates are best matched for M–N bond lengths of 2.10Å (81) whereas high–spin Ni^{2+} should fit perfectly into the cavity of the sarcophaginates (81).

In order to make the tetraazamacrocycles rigid, Hancock et al. (82,83) have added bridging ethylene groups between the nitrogen donors (Fig. 1.7.1), to give a piperazine–like structure. The bridging groups tends to increase metal ion selectivity based on the match between cavity size and metal ion size (83).

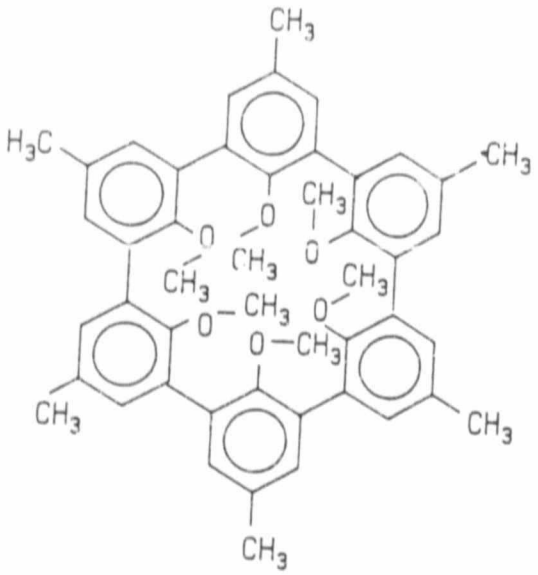

Spherand

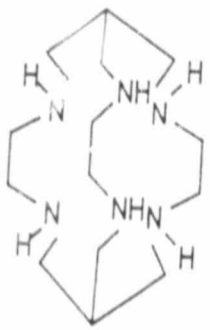

Sarcophagine

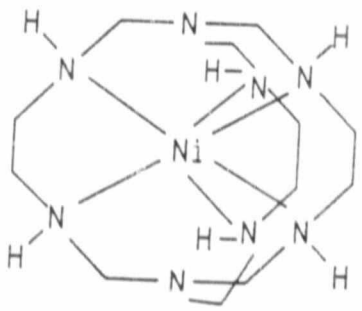

Sepulchrate

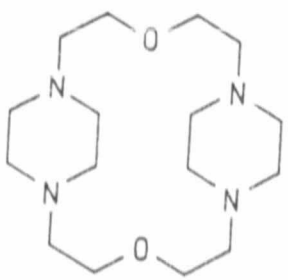

$(C_2)_2$-18-aneN_4O_2

Fig. 1.7.1 Structures of some rigid macrocyclic ligands.

Smaller rings are more rigid than larger macrocyclic rings and thus rigidity in larger macrocycles can be achieved by incorporating the smaller ring such as the nine–membered ring into larger units. The 9–aneN_3 type of rings and other nine–membered rings such as 9–aneS_3, 9–aneN_2O and 9–aneN_2S are known to display size–selectivity (84–87).

Part of this work involves the synthesis of bridged ligands in which the 9–aneN_2O units are incorporated into larger macrocycles.

1.8 AIMS OF THIS STUDY

It is apparent from the foregoing discussion that there are three properties that control metal–ion size–selectivity:

1. The size of the chelate ring formed. By increasing the chelate ring from a five– to a six–membered chelate ring, the ligand selectivity for small metal ions increases.
2. The neutral oxygen donor. Addition of neutral oxygen donor bearing groups to ligands will increase the ligand selectivity for large metal ions.
3. Addition of extra bridging groups between nitrogen donors increases the rigidity of macrocyclic ligands. Metal–ion selectivity depends on the match between the macrocyclic cavity and the size of the metal ion.

The main emphasis of this study is the design and synthesis of novel macrocyclic ligands containing both oxygen and nitrogen donors, and containing in some cases also pendent donor groups bearing one or more oxygen donors. The stabilities of the complexes of these ligands with a variety of metal ions is measured. In this way the size–selective properties of the neutral oxygen donor can be investigated further.

The second part of this work involves the use of properties (1) and (3) above. Attempts are made to synthesize macrocyclic ligands of a suitable cavity size that will form strong complexes with the metal–ion Pb^{2+}. The stabilities of these ligands with a variety of metal ions is measured.

The third part of this work involves the determination of the crystal structure of [K(BHE—18–aneN_2O_4)]Cℓ and [K(BHEE–18–aneN_2O_4)]I. Since the latter ligand is sterically more hindered than the former ligand comparison of the two structures was of interest. The crystal structure of [Ba(BHEE–18–aneN_2O_4]I_2 was also determined, in an attempt to understand the fact that Ba^{2+} is the only metal ion which forms a more stable complex with BHEE–18–andN_2O_4 than with BHP–18–aneN_2O_4.

CHAPTER 2

EXPERIMENTAL

2.1 INSTRUMENTATION

The products were characterized by nuclear magnetic resonance (N.M.R.), melting points (m.pt) and C,H and N analysis. The N.M.R. spectra were recorded either on a Varian EM 360 (60MHz) or the Bruker AC–200 spectrometer. All melting points were measured on a Reichert hot stage microscope melting point apparatus and are uncorrected. The C,H,N and O microanalysis were determined either at the C.S.I.R. or at Galbraith Laboratories, Inc.

2.2 MATERIALS

The metal ion solutions used in stability constant studies were prepared from AR nitrate salts. The list of materials used is given below

Material	Manufacture
Propylene Oxide	Hopkin and Williams Ltd.
1,2–bis–(2–chloroethoxy)–ethane	Fluka
2–(2–aminoethoxy)ethane	Aldrich Chemical Company Inc.
N–(2–Bromethyl)phthalimide	Aldrich Chemical Company Inc.
N–(3–Bromopropyl)phthalimide	Aldrich Chemical Company Inc.
Kryptofix–2,1	Merck

2.3 SYNTHESIS

2.3.1 N,N'–bis(2–hydroxypropyl)–1,4,10–trioxa–7,13–diazacyclo–pentadecane(DHP–15–aneN_2O_3)

To a solution of 1,4,10–trioxa–7,13–diazacyclopentadecane (1g; 4.6mmol) dissolved in absolute ethanol (25ml) was added excess propylene oxide (1.08g; 18.6mmol). The solution was stoppered and stirred at room temperature for one week. The solvent and excess propylene oxide were removed using a rotary evaporator to give a brown oil. The product was distilled at 150 – 155°C under reduced pressure to give a clear oil, which crystallized out on standing. Yield 68% based on the mass of the parent amine.

M.pt	:	44 – 45°C
N.M.R. $\delta(CDCl_3$; 60MHz)	:	1.06 (6H,d,CH_2)
		2.18 – 2.93 (12H,m,–C$\underline{H}_2$–N)
		3.63 (14H,m,–C$\underline{H}_2$–O and C$\underline{H}$OH)
		4.20 (2H,s,O$\underline{H}$)
C,H,N microanalysis	:	
(found; calculated		C (57.46; 57.46)
for $C_{16}H_{34}N_2O_5$)		H (10.41; 10.25)
		N (8.25; 8.38)

2.3.2 1,4–dioxa–7,10,13–triazacyclopentadecane(15–aneN_3O_2)

The cyclic tritosylate of 15–aneN_3O_2 was prepared by the method of Richman and Atkins (88). It was detosylated as follows: A solution of the tritosylate precursor (18g; 26.5mmol) in a mixture of hydrobromic acid

(590ml) and acetic acid (400ml) was heated under reflux (100 – 105°C)* with stirring for 48 hours. The solution was filtered through glass wool while hot and concentrated under reduced pressure to approximately 100ml. The residue was dissolved in 96% ethanol. Addition of ether precipitated the trihydrobromide salt which was recrystallized from methanol. Yield, 33.6%

*Refluxing the solution at temperatures higher than 100 – 105°C cleaved the macrocyle to yield the trihydrobromide salt of diethylenetriamine.

Melting point	:	240 – 242°C
N.M.R. $\delta(D_2O; 60MHz)$	:	3.46 (12H,m,–C<u>H</u>$_2$–N)
		3.76 (8H,m–C<u>H</u>$_2$–O)
C,H,N and O microanalysis		
(found; calculated	:	C (26.44; 26.11)
for $C_{10}H_{23}N_3O_2 \cdot 3HBr$)		H (5.99; 5.70)
		N (9.09; 9.13)
		O (6.67; 6.96)

2.3.3 <u>7,10,13–tris(2–hydroxypropyl)–1,4–dioxa–7,10,13–triaza–cylopentadecane(THP–15–aneN_3O_2)</u>

The free base of 15–aneN_3O_2 was obtained by dissolving the trihydrobromide salt in 10M NaOH and extracting it from chloroform. The chloroform was removed using a rotary evaporator to give a clear oil which recrystallized on refrigeration. To a solution of 15–aneN_3O_2 free base (1g; 4.60mmol) in absolute ethanol (25ml) was added propylene oxide (3ml; 42.8mmol). The solution was stoppered and stirred at room temperature for five days. The ethanol was evaporated to obtain a viscous

liquid which was distilled at 130 – 134°C under reduced pressure. A pale yellow oil was obtained. Yield, 77.8%.

N.M.R. $\delta(CDCl_3; 60MHz)$	:	1.1 (9H,d,–C<u>H</u>$_3$)
		2.15 – 2.9 (18H,m,–C<u>H</u>$_2$–N)
		3.6 (11H; m,–O–C<u>H</u>$_2$ and –O–C<u>H</u>)
		4.5 (3H, broad s, OH)
C,H and N microanalysis		
(found; calculated	:	C (57.07; 58.28)
for $C_{19}H_{41}N_3O_5$)		H (10.20; 10.55)
		N (10.49; 10.73)

2.3.4 <u>1,4–dioxa–7,10,13,16–tetraazacyclooctadecane(18–aneN_4O_2)</u>

The cyclic tetratosylate was prepared by the condensation method of Richman and Atkins (88). The detosylation was carried out as described for 15–aneN_3O_2. Yield, 48%

Melting point	:	228 – 230°C
N.M.R. $\delta(D_2O; 60MHz)$	:	3.56 (16H,m,–C<u>H</u>$_2$–N)
		3.7 (8H,m,–C<u>H</u>$_2$–O)
C,H and N microanalysis		
(found; calculated	:	C (23.93; 24.68)
for $C_{12}H_{28}N_4O_2.4HBr$)		H (5.31; 5.52)
		N (9.40; 9.59)

2.3.5 7,16–bis(O–(2–hydroxyethyl)–ethoxy)–1,4,10,13–tetra–oxa–7,16–diazacyclo–octadecane (BHEE–18–aneN_2O_4)

The method employed was similar to that reported by Gatto and Gokel (89) for other N–substituted 18–aneN_2O_4 ligands, involving the condensation of 2–(2–aminoethoxy)ethanol with 1,2–bis(2–iodoe–thoxy)ethane. Recrystallization from tetrahydrofuran (THF) gave the KI complex as white crystals. Yield, 7.2%

Melting point	:	97 – 100°C
N.M.R. ($CDCl_3$; 60MHz)	:	3.66 (30H,m,–C<u>H</u>$_2$–O and –O<u>H</u>)
		2.60 (12H,m,–C<u>H</u>$_2$–N)
C,H,N and O microanalysis		
(found; calculated	:	C (39.94; 39.73)
for $C_{20}H_{42}N_2O_8 \cdot KI$)		H (7.33; 7.00)
		N (4.36; 4.63)
		O (21.25; 21.17)

2.3.6 4,7–bis(aminoethyl)–1–oxa–4,7–diazacyclononane(BAE–9aneN_2O)

The synthesis is based on the method of Billo and Patel (90) modified by the use of a solvent.

To the free base of 9–aneN_2O (prepared as given for 15–aneN_3O_2)(1.9g; 14.6mmol) in acetonitrile (100ml) was added K_2CO_3 (10.1g; 73.1mmol) and N–(2–bromoethyl)phthalimide (7.4g; 29.2mmol). The solution was stirred and refluxed for 24 hours. The K_2CO_3 was filtered off and the acetonitrile was removed using a rotary evaporator. Hydrochloric acid (conc., 100ml) was added to the residue and refluxed for 6 – 8 hours. The

solution was cooled and the phthalic acid filtered off. The filtrate was made strongly basic with NaOH. The product was extracted from chloroform which was dried over anhydrous $MgSO_4$. Evaporation of the chloroform gave a yellow oil which was distilled between 60 – 65°C under reduced pressure to give a clear oil which was found to be hygroscopic. Yield, 60%.

N.M.R. $\delta(CDCl_3$; 200MHz) : 1.62 (5H,s,–N<u>H</u>$_2$ and <u>H</u>$_2$O)
2.75 (16H,m,–C<u>H</u>$_2$–N)
3.75 (4H,m,–C<u>H</u>$_2$–O)

C,H, N microanalysis analysed for $[Cu(BAE–9aneN_2O)](NO_3)_2 \cdot 0.5H_2O$

(found; calculated for $CuC_{10}H_{24}N_6O_7 \cdot 0.5H_2O$) : C (29.05; 29.09)
H (5.95; 6.10)
N (20.81; 20.36)

2.3.7 <u>4,7–bis(aminopropyl)–1–oxa–4,7–diazacyclononane(BAP–9aneN$_2$O)</u>

The method was as described for the above ligand except that N–(3–bromopropyl)phthalimid was used instead of 2–(bromo–ethyl)phthalimide and hydrolysis in acid was refluxed for 24 hours. The product was distilled at 115 – 118°C under reduced pressure to give a clear oil. Yield 58.8%.

N.M.R. $\delta(CDCl_3$; 60MHz): 1.5 (8H,m,–N<u>H</u>$_2$ and CH_2–C<u>H</u>$_2$–CH_2)
2.7 (16H,m,–C<u>H</u>$_2$–N)
3.8 (4H,m,–C<u>H</u>$_2$–O)

C,H and N microanalysis analysed for $[Cu(BAP–9aneN_2O)](NO_3)_2$

(found; calculated for $CuC_{12}H_{28}N_6O_7$) C (33.23; 33.37)
H (6.64; 6.53)
N (19.67; 19.46)

2.3.8 4,8–bis(aminoethyl)–1–oxa–4,8–diazacyclodecane(BAE– 10aneN$_2$O)

The method employed was as described for the ligand BAE–9aneN$_2$O except that 10–aneN$_2$O (prepared as described for 15–aneN$_3$O$_2$) was used instead of 9–aneN$_2$O. The hydrolysis in acid involved refluxing for 24 hours. The product was distilled at 110 – 113°C under reduced pressure to give a clear oil which turned yellow on standing. The product was found to contain 0.5 H$_2$O. Yield 60%

N.M.R. δ(CDCl$_3$; 200MHz) : 1.5 (2H,m,–CH$_2$–C<u>H$_2$</u>–CH$_2$)
1.85 (5H,s,–N<u>H$_2$</u> + <u>H$_2$</u>O)
2.4 – 3.0 (16H,m,–C<u>H$_2$</u>–N)
3.7 (4H,m,–C<u>H$_2$</u>–O)

C,H and N microanalysis analysed for [Cu(BAE–10aneN$_2$O)](NO$_3$)$_2$.H$_2$O
(found; calculated : C (30.11; 30.31)
for CuC$_{11}$H$_{28}$N$_6$O$_8$) H (6.14; 6.47)
N (19.20; 19.28)

2.4 DETERMINATION OF STABILITY CONSTANTS

2.4.1 Potentiometric Titrations

The stability constants were determined by potentiometric titration in cells thermostatted at 25°C. The potentials were recorded on a Radiometer PHM84 research pH meter using Radiometer GK2401C glass electrodes with a Ag/AgCl reference electrode and a salt bridge to eliminate junction potentials. All measurements were made in an aqueous

medium of ionic strength 0.1M using sodium nitrate as background electrolyte. The glass electrodes were calibrated by recording the potentials as a function of calculated pH in the pH range 2 to 11.

The solution of the protonated ligand was standardized with a standard solution of approximately 0.05M sodium hydroxide in 0.05M sodium nitrate. The solution of the unprotonated ligand was titrated with a standard solution of approximately 0.05M nitric acid in 0.05M sodium nitrate. The pKa values were also determined from these titrations. For the determination of the stability constants at least three separate titrations were carried out for each metal ion with each ligand using different ligand to metal ratios. All the ligands appeared to equilibrate rapidly with the metal ions during the titrations. For the ligands which were obtained as hydrobromide salts, the bromide ions were removed from the stock solution by addition of the calculated amount of silver nitrate, followed by filtration and restandardization. This solution was then used for the determination of the stability constant of the Pb^{2+} ion.

The formation constants were calculated using the program EQUILIBRIA (91) and MINIQUAD (92). All the experimental data together with the plots of the experimental and calculated values of $\bar{n}$ (the average number of ligands bound per metal ion) versus $-\log[L]$ are given in the supplementary material on microfiche.

2.4.2 N.M.R. Spectroscopy

The N.M.R. spectra were recorded on a Bruker AC200 FT NMR spectrometer (96). All samples were measured in 10mm–o.d. N.M.R. tubes with a capillary insert containing a chemical shift reference (1M

CsCl; RbI and NaCl in water placed in different capillaries). All measurements were made at the probe temperature of approximately 23°C. At the field strength of 4.T ^{23}Na resonates at 52.94 MHz ^{87}Rb at 65.49MHz and ^{133}Cs at 26.25MHz.

The following solutions were prepared in dry methanol:–

0.0100M CsCl	and 0.00933M CsCl	in ~0.02M ligand
0.01867M RbI	and 0.01922M RbI	in ~0.04M ligand
0.0100M $NaNO_3$	and 0.00933M $NaNO_3$	in ~0.02M ligand

The ligands used were BHP–18–aneN_2O_4; 15–aneN_3O_2 and THP–15aneN_3O_2. Typically, 3ml of the metal solution was placed in the tube. The position of the metal peak in methanol relative to the reference peak was determined. Thereafter, small increments of the ligand solution were added to the tube and a spectrum recorded after each addition using (^{133}Cs; ^{87}Rb and ^{23}Na).

The stability constant for the complex was estimated from the shifts in position of the peak due to the complex relative to the reference peak. The data are given in Appendix 1.

The determination of the stability constant is based on the equilibrium:

$$M + L \rightleftharpoons ML$$

metal macrocyle complex

The equation $$\bar{n} = \frac{ni - no}{n\infty - no}$$

gives the correlation between the chemical shifts of the probe cation and

the extent to which the complex has been formed ($\bar{n}$), where

n_i = peak position after iml of ligand solution has been added to the metal solution,

n_o = peak position of the metal solution alone,

n_∞ = peak position after an infinite amount of ligand has been added to the metal solution.

The stability constant (K1) for the complex may be calculated from the equation

$$K1 = \frac{[ML]}{[M][L]}$$

where $[ML] = \bar{n}\Sigma M$;

$[L] = \Sigma L - [ML]$

$[M] = \Sigma M - [ML]$

The total metal and ligand concentrations are given by the equation

$$\Sigma L = \frac{[L].(\text{volume of L})}{(\text{volume of L} + \text{volume of M})}$$

$$\Sigma M = \frac{[M].(\text{volume of M})}{(\text{volume of L} + \text{volume of M})}$$

L = macrocycle solution; M = metal solution alone.

2.5 X–RAY CRYSTALLOGRAPHIC STUDIES

2.5.1 Preparation of crystals

(a) [K(BHE–18–aneN_2O_4)]Cl

A 1:1 mixture of potassium chloride and BHE–18– aneN_2O_4, prepared by the method of Kulstad and Malmsten (97), was mixed in water. The water was removed using a rotary evaporator. Recrystallization from a minimum quantity of ethanol gave pale

yellow crystals. M.pt.: 172 – 173°C.

C,H and N microanalysis, found: C, 45.25; H, 8.24; N, 6.23%. Calculated for: C, 45.22; H, 8.06; N, 6.59%

(b) [K(BHEE–18–aneN_2O_4)]I

The synthesis of the ligand gives the KI complex. These crystals were found to be twinned as obtained by recrystallization from THF. Recrystallization from benzene gave non–twinned crystals which were used for the crystallographic study.

(c) [Ba(BHEE–18–aneN_2O_4]I

A 1:1 mixture of BHEE–18–ane$N_2O_4 \cdot$KI and $BaI_2 \cdot 2H_2O$ was made up in water. The water was evaporated using a rotary evaporator. Recrystallization from ethanol and iso–proponal gave crystals that were twinned. A second attempt to recrystallize the crystals from absolute ethanol gave non–twinned crystals which were used for the crystallographic study. M.pt.: 220°C(d).

C,H and N microanalysis for BHEE–18–ane$N_2O_4 \cdot BaI_2 \cdot 3H_2O$, found: C, 27.22; H, 5.44; N, 2.93%. Calculated for: C, 27.18; H, 5.47; N, 3.17%.

2.5.2 Data Collection

The data were collected at room temperature on an Enraf–Nonius CAD–4 diffractometer using graphite–monochromated MoKα radiation (0.71073Å). The cell dimensions were obtained from least square

refinements of 25 high theta reflections. An ω–2Θ scan mode was used with a scan width of $0.6 + 0.35 \tan\Theta$ and a variable scan speed. Three standard reflections were monitored and showed no significant variation over the data collection. Lp and absorption corrections were applied to the data according to the method of North et al. (93). The crystal data and data collected parameters for the structures are given in Table 5. The observed densities of the crystals were obtained using the flotation method. In each case a pair of solvents from the following list was used: hexane, carbontetrachloride, 1,2–dibromoethane.

2.5.3 Structure Determination

Patterson and Fourier techniques were used to determine the atomic co–ordinates. The final atomic coordinates were added by least–square refinement using anisotropic temperature factors for non–hydrogen atoms, from which bond lengths and bond angles were calculated. Hydrogen atoms were either placed using different Fourier maps or placed in geometrically calculated positions, C–H = 1.08Å. Scattering factors for the heavy metal atoms were obtained from "International Tables of Crystallography", (94). The structures were solved and refined using the program SHELX (95) either on the CDC CYBER 174/750 of the C.S.I.R. or the IBM microcomputer with a definicon board. The final fractional coordinates, the bond lengths and angles, and the anisotropic temperature factors for the structures reported are given in Appendix 2. Tables of calculated and observed structure factors are given in the supplementary material on microfiche. Figure 2.5.3 a – d gives the atomic numbering scheme of the reported structures

Table 5 Details of the Crystallographic Analysis of [K(L ,EE–18–ane N_2O_4] I and [K(BHE–18–ANE N_2O_4)]Cl

Formula	$C_{20}H_{42}N_2O_8KI$	$C_{16}H_{34}N_2O_6$ KCl
Molecular weight/gmol^{-1}	604.65	425.01
Crystal System	Monoclinic	Monoclinic
Space Group	$P2_1/c$	C2/c
Cell Dimensions		
a/Å	8.805(4)	13.331(3)
b/Å	14.221(2)	15.716(2)
c/Å	21.957(3)	11.577(4)
β/deg	100.27(2)	117.69(3)
V/Å^3	2705.16	2147.53
Z	4	4
d obs/gcm^{-3}	1.46	1.32
d calc/gcm^{-3}	1.48	1.32
F(000)	1248	908
Crystal colour	Colourless	Pale Yellow
Crystal Dimensions/mm	0.14x0.21x0.30	0.25x0.50x0.50
Theta Range/deg	$2 \leq \Theta \leq 27$	$2 \leq \Theta \leq 30$
Range of h, k, l	±11, +18, +28	±18, +22, +16
Scan Speed Range/ deg min^{-1}	1.4 – 5.5	0.9 – 5.5
No. of reflections measured	6289	3383
No. of unique data	4701	2877
Rint	0.0171	0.0106
No. of data used	2828	2325
Cut of criteria	$[F>3\sigma(F_o)]$	$[F>4\sigma(F_o)]$
Abs coeff (Uγ)cm^{-3}	12.70	3.55
Range of Transmission Factors	94.3 – 100.0%	93.8 – 100.0%
Final R	0.054	0.029
No. of Parameters	297	171
Residual Density/e Å^{-3}	0.89	0.22

Table 5 continued — Details of the Crystallographic Analysis of $[Ba(BHEE-18-aneN_2O_4)]I_2 \cdot 3H_2O$

Formula	$C_{20}H_{42}N_2O_8BaI_2 \cdot 3H_2O$
Molecular weight/gmol^{-1}	883.74
Crystal System	Monoclinic
Space Group	C2/c
Cell Dimensions	
a/Å	11.378(1)
b/Å	15.682(2)
c/Å	18.222(2)
β/deg	96.28(8)
V/Å^3	3231.87
Z	4
dobs/g cm^{-3}	1.80
dcalc/gcm^{-3}	1.74
F(000)	1728
Crystal colour	Colourless
Crystal Dimensions/mm	0.35x0.25x0.25
Theta Range/deg	$2 \leq \Theta \leq 30$
Range of h, k, ℓ	$\pm 15, +22, +25$
Scan Speed Range/ deg min^{-1}	1.3 – 5.5
No. of reflections measured	4992
No. of unique data	4340
Rint	0.0145
No. of data used	3494
Cut of criteria	$[F > 4\sigma(F_o)$
Abs coeff ($U\tau$)cm^{-3}	29.74
Range of Tranmission Factors	92.9 – 100.0%
Final R	0.032
No. of Parameters	177
Residual Density/e Å^{-3}	0.98

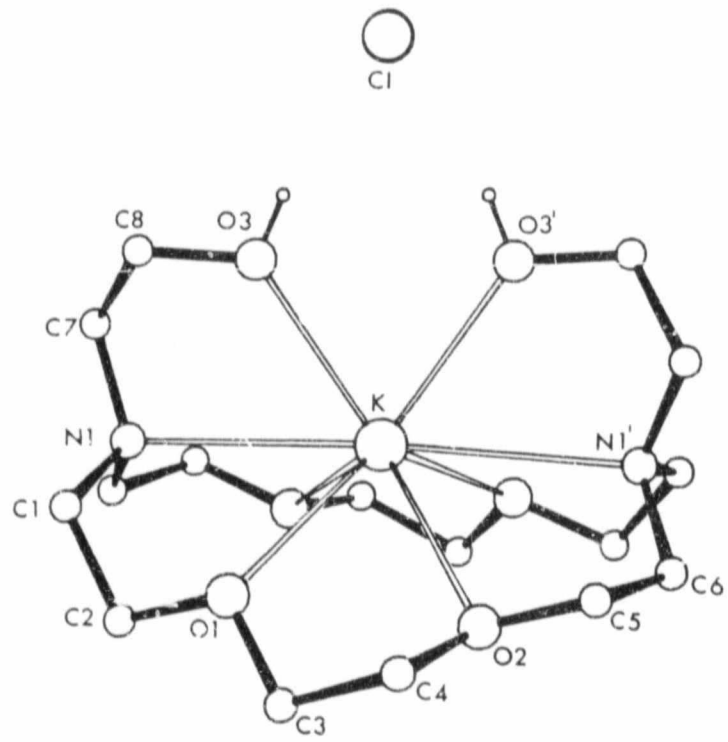

Fig. 2.5.3a The structure and atomic numbering scheme of $[K(BHE-18-aneN_2O_4)]Cl$

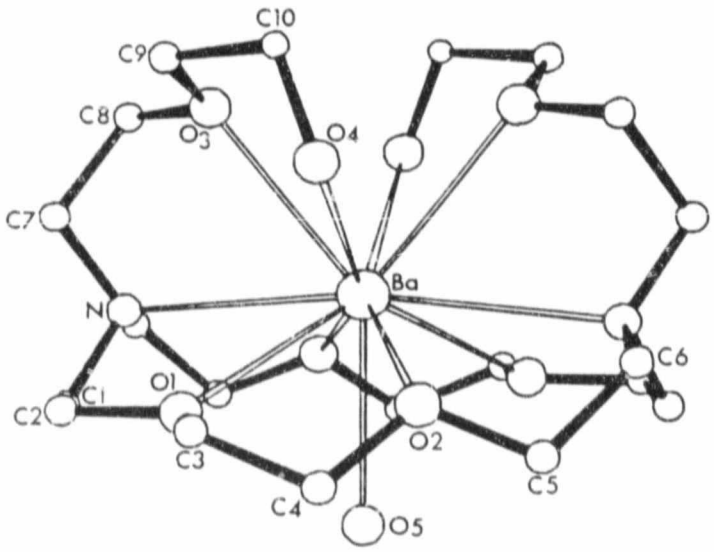

Fig. 2.5.3b The structure and atomic numbering scheme of $[Ba(BHEE-18-aneN_2O_4)]I_2 \cdot 3H_2O$

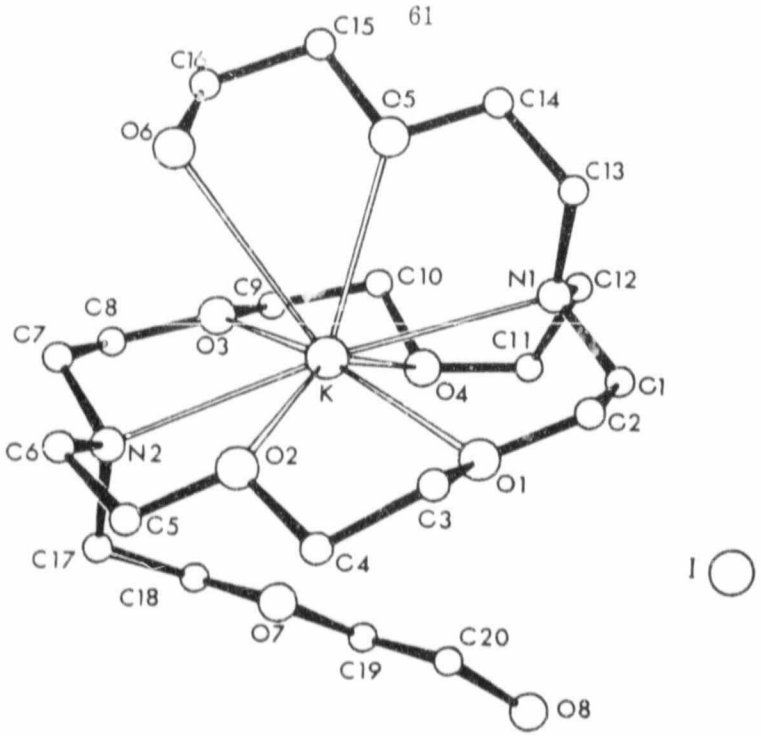

Fig. 2.5.3c The structure and atomic numbering scheme of [K(BHEE–18–aneN_2O_4)]I–major component

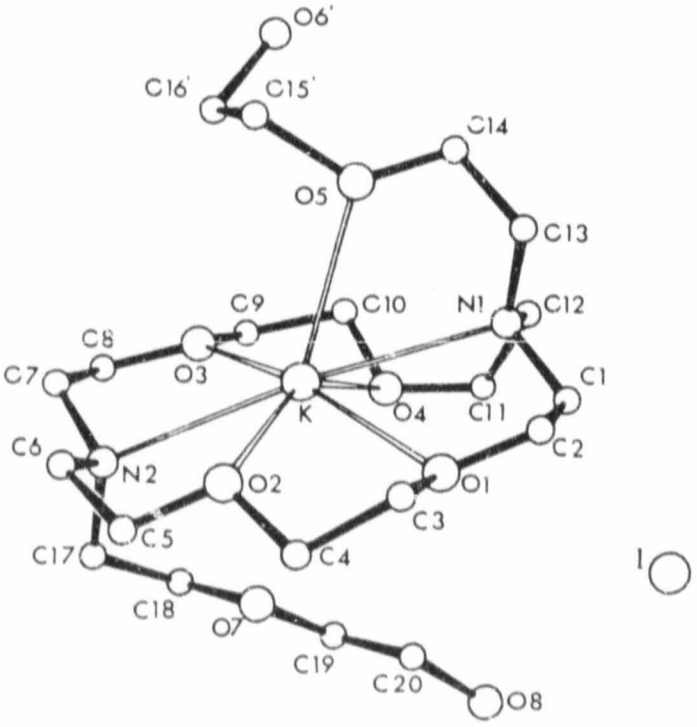

Fig. 2.5.3d The structure and atomic numbering scheme of [K(BHEE–18–aneN_2O_4)]I–minor component

CHAPTER 3

RESULTS AND DISCUSSION

3.1 THE CONTRIBUTION OF CAVITY SIZE TO METAL ION SIZE–SELECTIVITY

The neutral oxygen donor has for some time been of considerable interest because of its occurrence in crown ethers (2), and more recently because of its occurrence as alcoholic and ethereal oxygens in side arms on ligands such as the "lariat ethers" (53,89). An important idea in crown ether chemistry has been that of "hole–size–selectivity" (2), that is, the idea that metal ion size–selectivity is governed by the match between the size of the metal ion and the cavity in the centre of the macrocycle. More recent evidence (38) indicates that factors other than the macrocyclic cavity may be responsible for controlling metal ion size–selectivity, and that much of the observed behaviour of these macrocycles is the property of the neutral oxygen donor rather than the macrocyclic cavity. However, there does appear to be a contribution from cavity size, and in order to allow for a more detailed analysis of the role of the macrocyclic cavity, the study of the complexing properties of the ligand DHP–15–ane N_2O_3 is reported. This ligand is similar to DHP–18–ane N_2O_4 except that DHP–15–ane N_2O_3 has a fifteen membered ring, whereas DHP–18–ane N_2O_4 has an eighteen membered ring. This difference will thus allow for the evaluation of the effect of macrocyclic ring size on the ability of the ligand to distinguish between metal ions on the basis of size. The structures of the ligands discussed are shown in Fig. 3.1.1.

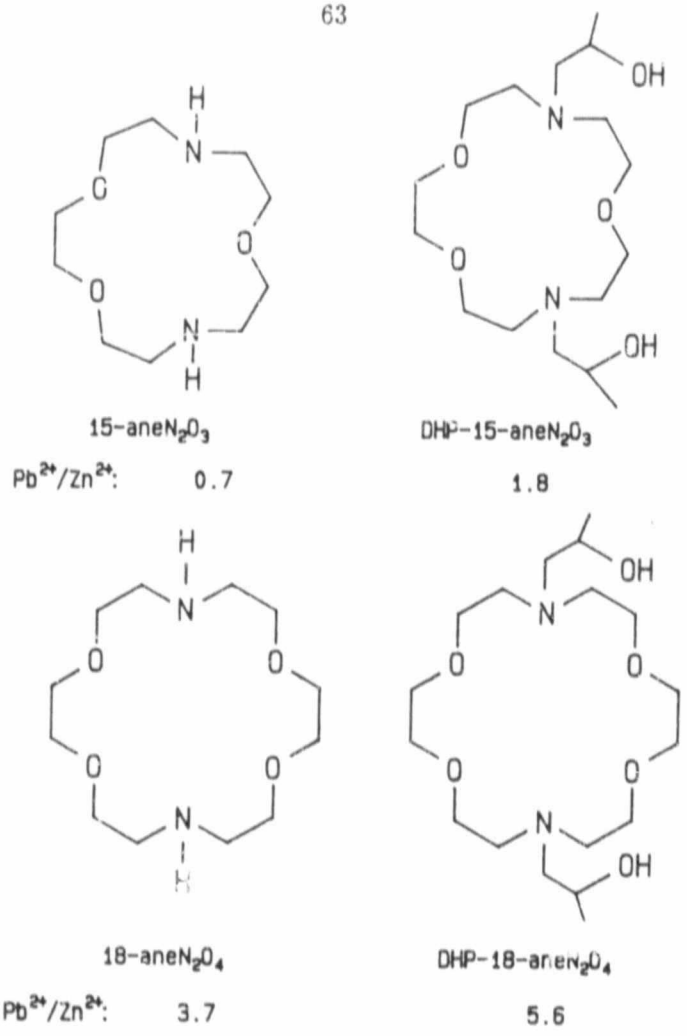

Fig. 3.1.1 Structures of the ligands discussed in this section

The formation constants for a variety of metal ions with the ligands DHP–15–ane N_2O_3 are given in Table 6, together with those of some structurally similar ligands for comparison. Comparison of the complexing properties of DHP–15–ane N_2O_3 and DHP–18–ane N_2O_3 appears to indicate that there is an effect of macrocyclic ring size on complex stability. Thus, in the case of DHP–18–ane N_2O_4 which has an eighteen–membered ring, the order of complex stability amongst the alkaline earth metal ions is $Ba^{2+}>Sr^{2+}>Ca^{2+}$. In the case of DHP–15–aneN_2O_3, which has a smaller fifteen–membered ring, the order has been reversed to $Ca^{2+}>Sr^{2+}>Ba^{2+}$. In other words, the large Ba^{2+} ion coordinates better to the 18–membered ring

whereas the smaller Ca... coordinates better to the 15–membered ring. For smaller metal ions such as Cu^{2+} and Zn^{2+}, the complexes found with DHP–15–ane N_2O_3 are relatively more stable than those formed with DHP–18–ane N_2O_4. However, in increasing the ring size of DHP–15–aneN_2O_3 to give DHP–18–ane N_2O_4, an extra ethereal oxygen donor has also been added. As mentioned in Section 1.6 addition of neutral oxygen donor atoms to an existing ligand causes a drop in complex stability with small metal ions. The metal ions Ca^{2+} and Cd^{2+} are of almost the same size but there is a large difference in stability between the two complexes. This difference in complex stability can be explained in terms of hardness and softness. The softer metal ion Cd^{2+}, interacts much more strongly with the nitrogen donors whereas the hard Ca^{2+} has a low affinity for nitrogen and hence weaker M–N interactions.

The contribution of macrocyclic ring size to metal ion size selectivity becomes more apparent when comparisons are made of the Pb^{2+}/Zn^{2+} selectivity, since the Zn^{2+} ion is much smaller than the Pb^{2+} ion. This is shown in Fig. 3.1.1. When pendent donor groups bearing neutral oxygen donors are added, as in passing from 15–ane N_2O_3 to DHP–15–ane N_2O_3 or 18–ane N_2O_4 to DHP–18–ane N_2O_4, there is an increase in the Pb^{2+}/Zn^{2+} selectivity of one to two log units. On the other hand, addition of a single oxygen donor into a macrocyclic ring, as in passing from 15–ane N_2O_3 to 18–ane N_2O_4, the increase in Pb^{2+}/Zn^{2+} selectivity is considerably larger, of the order of three to four log units. The conclusion is that, although oxygen donors which are not part of a macrocyclic ring produce similar results on selectivity to those which are part of a macrocyclic ring (32,62), addition of oxygen donors into the macrocyclic ring has a considerably larger effect on metal ion size selectivity which must be taken into account in ligand architecture.

Examination of other diamine ligands, as those shown in Fig. 3.1.2, appears to support the above results.

Table 6 The formation constants of a variety of metal ions with the ligand DHP–15–ane N_2O_3, and those of some structurally similar ligands for comparison. Metal ions are arranged in increasing size.

	15–ane N_2O_3[b]	18–ane N_2O_4[b]	DHP–15–ane N_2O_3[a]	DHP–18–ane N_2O_4[b]
pKa_1			8.30(1)	
pKa_2			7.62(1)	
Ni^{2+}			4.13(1)	
Cu^{2+}	7.1	6.1	7.88(1)	5.97
Zn^{2+}	5.1	3.1	6.45(1)	3.0
Cd^{2+}	6.4	5.25	7.13(1)	7.64
Ca^{2+}		1.74	3.86(2)	3.59
Sr^{2+}		2.6	3.46(1)	4.05
Pb^{2+}	5.8	6.8	8.26(1)	8.57
Ba^{2+}		2.97	3.19(1)	4.65
Pb^{2+}/Zn^{2+}	0.7	3.7	1.8	5.6

[a] This work, 25°C, 0.1M $NaNO_3$

[b] Formation constants taken from Ref. 102.

Pb^{2+}/Zn^{2+} For each ligand is log $K_1(Pb^{2+})$ minus log $K_1(Zn^{2+})$

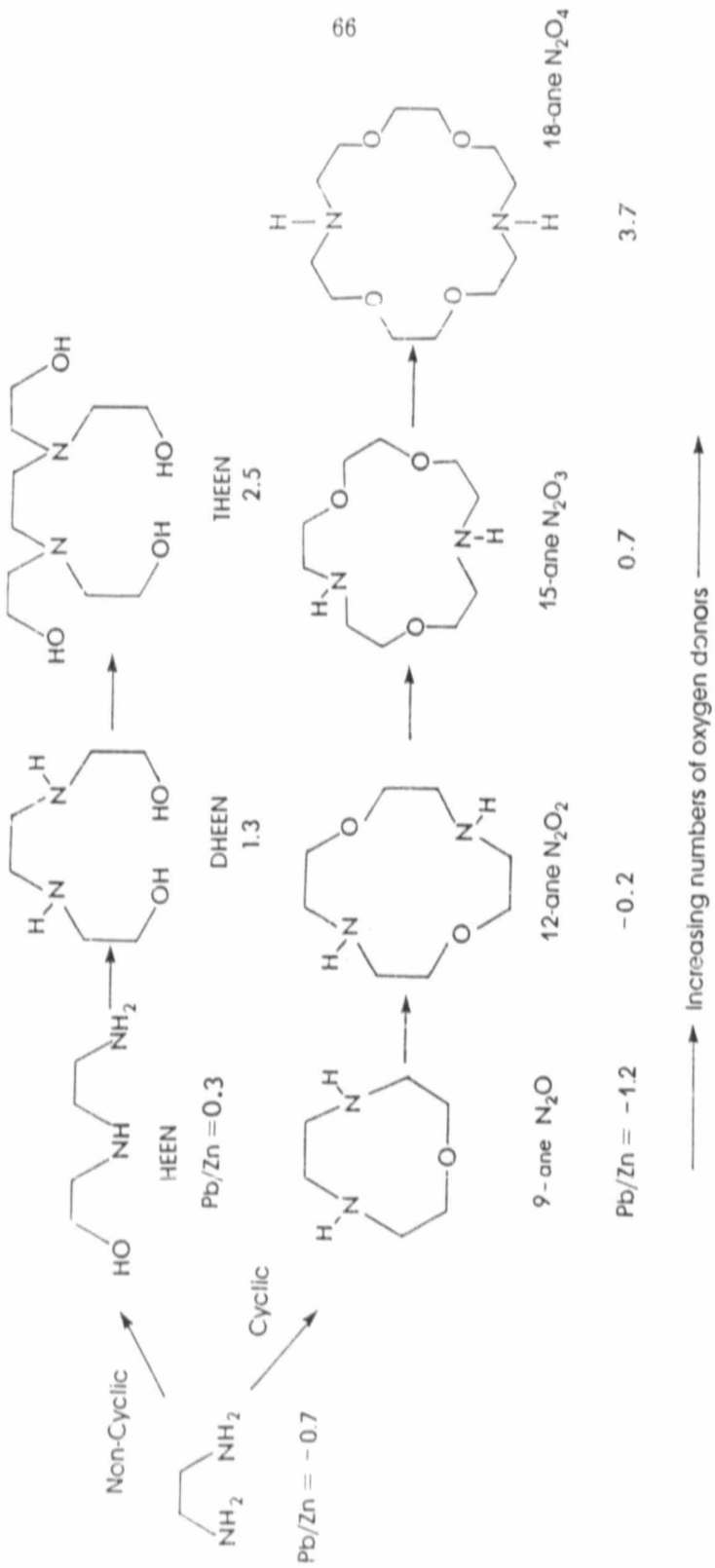

Fig. 3.1.2 Effect of macrocyclic cavity size on the Pb^{2+}/Zn^{2+} selectivity. The Pb^{2+}/Zn^{2+} selectivity is log K_1 Pb^{2+} minus log K_1 Zn^{2+}

The cavity of the 9–membered ring is best suited for small metal ions (126). The metal ion Zn^{2+} will thus fit better into the cavity of the 9–ane N_2O ring than Pb^{2+}, resulting in the formation of strong Zn^{2+} complexes compared to the Pb^{2+} complexes. Hence, the Pb^{2+}/Zn^{2+} selectivity is very much in favour of the small Zn^{2+}. This is not observed in the open–chain analogue, HEEN. In the case of the very much larger cavity, 18–aneN_2O_4, the Pb^{2+}/Zn^{2+} selectivity is considerably larger than for the open–chain analogue, THEEN. Macrocyclic cavities of intermediate size do not show Pb^{2+}/Zn^{2+} selectivities much different from their open–chain analogues. Thus, the size of the macrocyclic cavity does appear to contribute to the Pb^{2+}/Zn^{2+} selectivity with the 18–membered macrocycle producing much larger Pb^{2+}/Zn^{2+} selectivities than the smaller 15– and 12–membered macrocycle.

3.2 OXYGEN DONORS THAT FORM PART OF THE MACROCYCLIC RING

The oxygen donor macrocycles are well known for their ability to complex strongly with alkali and alkaline–earth metal ions. The nitrogen donor macrocycles complex more strongly with the transition and post–transition metal ions. With the mixed donor macrocycles containing both oxygen and nitrogen donors, it has been shown (48,107,108) that the presence of the nitrogen donor decreases the affinity of the ligand for the alkali and alkaline–earth metal ions but increases the interaction between the macrocycle and the transition metal ions, a fact which is accounted for by the concept of HSAB (13). On the other hand, most of the observed metal–ion size selectivity in these macrocycles has been accounted for by the presence of the neutral oxygen donor, and quite remarkable selectivity can be achieved by changing the number of oxygen donors and the size of the macrocyclic cavity (32,62,102).

The application of these mixed–donor macrocycles containing oxygen and nitrogen donors offer two advantages. The nitrogen donor affords some practical advantages for the introduction of pendent arms since the hydrogen atoms bonded to the nitrogen in these ligands can easily be substituted by convenient groups. The oxygen donor provides the desired metal ion size–selectivity in that the small metal ions, such as Cu^{2+} and Zn^{2+} are destabilized relative to the large metal ions in the presence of an oxygen donor. The ability to control metal ion size–selectivity is of interest in many areas. The toxic heavy metal ions like Cd^{2+}, Hg^{2+}, Pb^{2+} are large ions whereas the biologically important ions like Zn^{2+} and Cu^{2+} are small ions. Thus, ligands which display metal ion size–selectivity are of potential practical importance for therapeutic administration as well as for the control of metal ions in the environment. The main interest in this work is in the development of reagents for treating lead intoxication. The aim here is the removal of the large Pb^{2+} ion while minimally affecting the level of the essential small metal ion Zn^{2+}.

Recent work indicated (110) that addition of hydroxyalkyl arms to the macrocycle 12–ane N_3O to form THP–12–ane N_3O increased the Pb^{2+}/Zn^{2+} selectivity by only 1.24 log units. This was much less than the expected selectivity of 4.9 log units which was observed when hydroxyethyl arms were added to 14–aneN_4

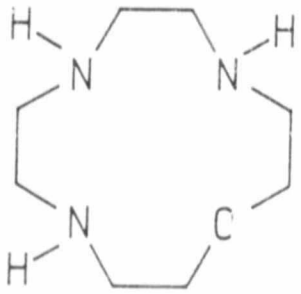

12-aneN_3O

Pb^{2+}/Zn^{2+}: 1.01

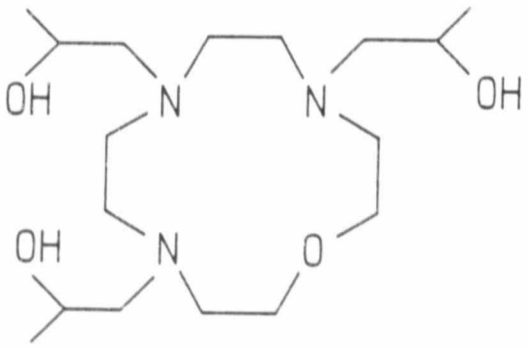

THP-12-aneN_3O

2.25

It has been shown (Section 3.1) that the addition of a single oxygen donor to a macrocyclic ring causes a much sharper increase in the Pb^{2+}/Zn^{2+} selectivity than when oxygen donors are added as pendent arms. The complexing properties of the ligand 15–ane N_3O_2 are thus reported. The macrocycle 15–ane N_3O_2 is similar to 12–ane N_3O except that it has an extra oxygen donor in the macrocyclic ring. The formation constants obtained with a variety of metal ions are given in Table 7 together with some literature values of other similar ligands for comparison.

The aim of this work was to evaluate further the effect of the neutral oxygen donor on size–selectivity patterns. In Fig. 3.2.1 the selectivities of a series of ligands for the large Pb^{2+} over the small Zn^{2+} are seen. It is clear that with the increase in the number of oxygen donors there is an increase in the Pb^{2+}/Zn^{2+} selectivity. It has been discussed in Section 1.6 that this selectivity pattern is not only observed when neutral oxygen donors are added to form a macrocyclic ring but it is also observed in open chain ligands and in ligands where the oxygen donor groups are added as pendent arms.

The effect of the neutral oxygen donor on size selectivity can be more closely analysed using the plots of change in complex stability, Δ log K, which occurs when a particular structural change is made to the existing ligand, as a function of the metal ion radius. Thus, in Fig. 3.2.2, a good linear relation is observed for Δ log K when 12–ane N_3O or 15–ane N_3O_2 is compared to DIEN as a starting ligand. A similar relationship was observed for Δ log K when cryptand–2,2,2 was compared to EN in Fig. 1.6.3. In general, the slope of a plot of Δ log K versus ionic radius increases with increase in the number of oxygen donors. The steeper the slope, the greater the Pb^{2+}/Zn^{2+} selectivity.

Table 7 Formation Constant (Log K_1) Values of Open–Chain Ligands and some Mixed–donor Macrocycles

	DIEN	12–ane N_3O	15–ane N_3O_2[a]	TRIEN	15–ane N_4O	18–ane N_4O_2[a]
pKa_1	9.84	10.18	9.29(1)	9.74	9.56	9.19(1)
pKa_2	9.02	8.56	8.50(1)	9.08	8.75	8.51(1)
pKa_3	4.23	1.43	2.12(1)	6.56	5.31	6.00(1)
pKa_4	–	–	–	3.25	–	2.56(1)
Ni^{2+}	10.5	12.15	8.93(1)	14.0	13.33	12.49(2)[b]
Cu^{2+}	15.9	15.85	15.27(1)	20.1	20.07	17.85(7)[b]
Zn^{2+}	8.8	10.53	8.85(1)	12.0	13.11	9.52(3)[b]
Cd^{2+}	8.3	10.78	10.05(1)	10.6	13.41	10.00(4)[b]
Pb^{2+}	7.56	11.54	10.07(1)	10.35	12.28	9.11(7)[b]
Pb^{2+}/Zn^{2+}	–1.2	1.0	1.2	–1.65	–0.83	–0.42

Protonation Constants for DIEN and TRIEN taken from Ref. 20.

Formation Constants for DIEN, TRIEN and 12–ane N_3O taken from Ref. 32.

Formation Constants for 15–ane N_4O taken from Ref. 131.

[a] This work, 25°C, 0.1M $NaNO_3$

[b] Additional constants found for these complexes are:

log K(MLH^{3+}): Ni^{2+} 17.14(2); Cu^{2+} 21.08(4); Zn^{2+} 14.88(6)

Cd^{2+} 16.02(2); Pb^{2+} 14.6(2)

log K(MLH_2^{4+}): Cu^{2+} 23.2(3); Zn^{2+} 20.28(8); Pb^{2+} 20.65(9)

Pb^{2+}/Zn^{2+} for each ligand is log K_1 (Pb^{2+}) minus log K_1 (Zn^{2+})

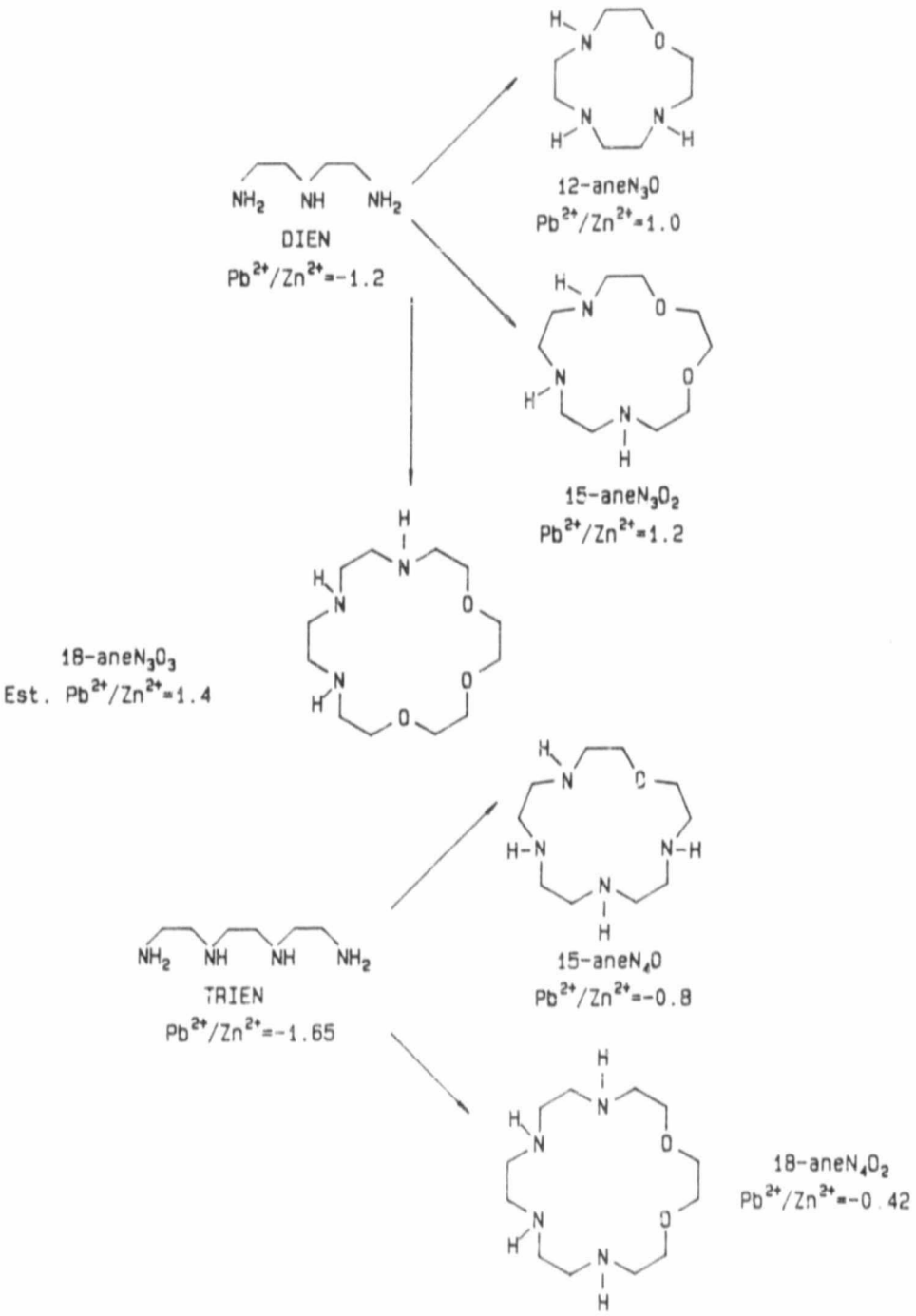

Fig. 3.2.1 The effect on the Pb^{2+} over Zn^{2+} selectivity as the number of oxygen donors are increased along the series of ligands. The selectivity, indicated as Pb^{2+}/Zn^{2+}, is simply the log K_1 for the Pb^{2+} complex minus log K_1 for the Zn^{2+} complex.

From inspection of the data in Table 7 and Fig. 3.2.2 it seems clear that metal complexes formed with the macrocycle 12–ane N_3O are more stable than the corresponding metal complexes formed with the larger macrocycle 15–ane N_3O_2. Thus increasing the ring size from 12– to a 15–membered ring leads to a decrease in complex stability. The Pb^{2+}/Zn^{2+} selectivity increases by only 0.2 log units when an extra 0–donor is added to 12–ane N_3O to form 15–ane N_3O_2. The low increase in the Pb^{2+}/Zn^{2+} selectivity in going from DIEN to 12–ane N_3O to 15–ane N_3O_2 can be associated with the smaller cavity sizes of these macrocycles. Attempts to synthesize the larger 18–membered macrocycle 18–ane N_3O_3 proved to be unsuccessful. However, the predicted Pb^{2+}/Zn^{2+} selectivity is estimated to be 1.4 log units, which could be higher, because of the presence of the 18–membered size ring. This selectivity, together with the 1.2 log units obtained with 15–ane N_3O_2, is lower than the 1.44 log units of EDTA, the current antidote used in the treatment of lead intoxication.

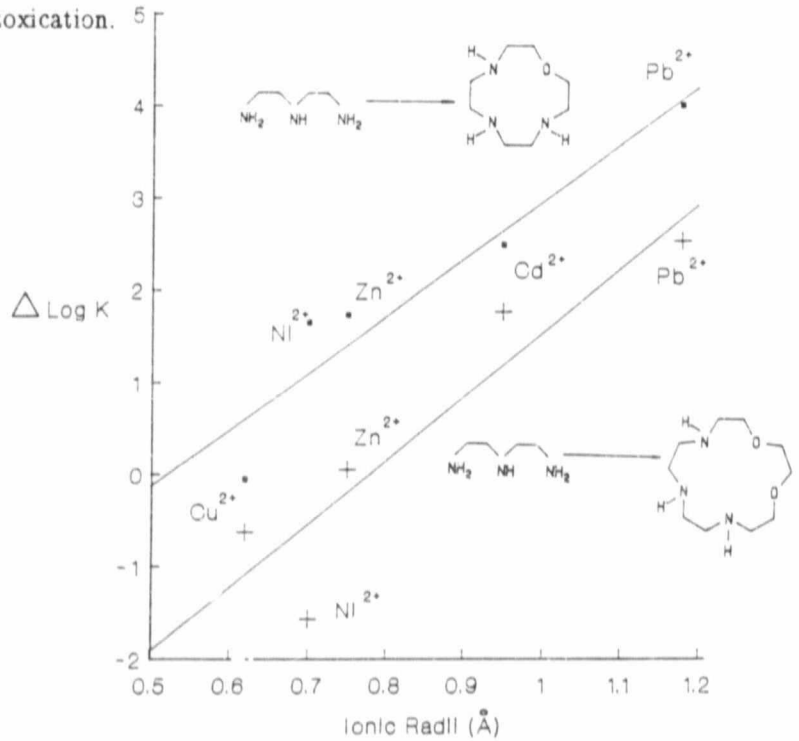

Fig. 3.2.2 The change in complex stability, Δ log K, as a function of metal ion radius as one ethereal oxygen is added to DIEN to give 12–ane N_3O or where two ethereal oxygen groups are added to DIEN to give 15–ane N_3O_2

Since the macrocycle 18–ane N_3O_3 could not be synthesized, it was decided to study the 18–membered macrocycle 18–ane N_4O_2. The formation constants for this macrocycle are given in Table 7. In Fig. 3.2.1 is shown the increase in Pb^{2+}/Zn^{2+} selectivity as the number of O–donors are increased from TRIEN to 15–ane N_4O to 18–ane N_4O_2. Although the Pb^{2+}/Zn^{2+} selectivity observed with 18–ane N_4O_2 is much higher than 15–ane N_4O and TRIEN the value is still very low, with the selectivity in favour of Zn^{2+} over Pb^{2+} . Inspection of Fig. 3.2.3, where the change in complex stability, Δ log K, for TRIEN going to 18–ane N_4O_2, is plotted against ionic radius, shows a linear relationship if the value of Pb^{2+} is excluded. A higher Pb^{2+}/Zn^{2+} selectivity would have been obtained if the Pb^{2+} value had been on the line. The reason the Δ log K value of Pb^{2+} lies off the curve is probably due to an effect of the lone pair of electrons. Recent evidence suggest (110) that two different forms of Pb^{2+} exist where the ionic radii differ.

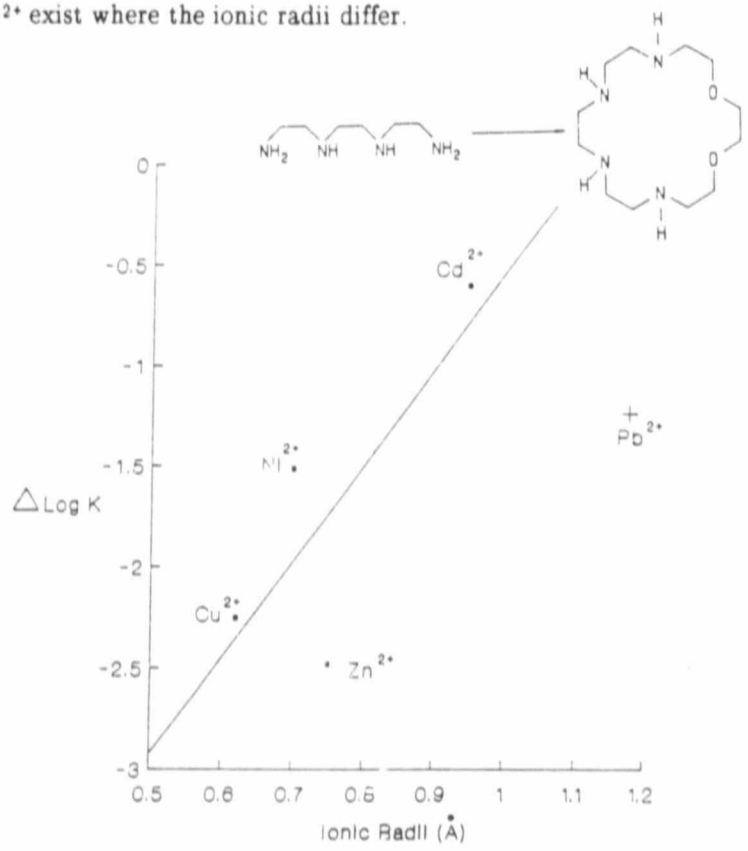

Fig. 3.2.3 The change in complex stability, Δ log K, as a function of metal ion radius as two ethereal oxygens are added to TRIEN to give 18–ane N_4O_2

This type of behaviour is analogous to the high– and low–spin states of Ni^{2+} which have two different ionic radii (109). In the case of Pb^{2+}, the lone pair of electrons can either be stereochemically "inactive" or stereochemically "active" (110). In the "inactive" form, the lone pair resides in the spherically symmetrical 6s orbital and the electrons are delocalized over the entire Pb atom. The donor electrons of the ligand will thus experience some repulsion, resulting in poor overlap between the M–L orbitals. This poor overlap will cause long ionic M–L bonds. In the active form, the lone pair resides in the sp_nd_m hybrid orbitals, where the electrons are localized. This results in effective overlap between metal and ligand orbitals, and thus shorter M–L bonds, i.e. the bonds will be more covalent (110). Shorter bond lengths in Pb^{2+} complexes mean that the Pb^{2+} ion has a smaller effective ionic radius. Thus, an "inactive" Pb^{2+} ion has a larger ionic radius than an "active" Pb^{2+} (110).

It has been shown (110) that the "active" and "inactive" forms of Pb^{2+} have a marked effect on complex stability. In the "active" form of Pb^{2+} the M–L bonds are covalent and hence these complexes have relatively large stabilities. The effect on complex stability is shown in Fig. 3.2.4.

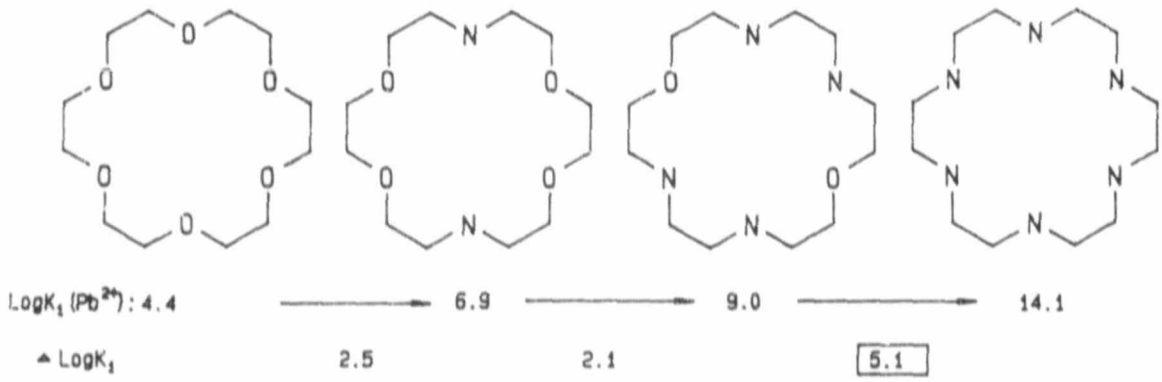

Fig. 3.2.4 The Pb^{2+} stability constant of the 18–membered macrocycle showing the increase in stability on substitution of two nitrogens on each step. The value in the box is the point at which a jump in stability occurs. Redrawn from Ref. 110.

Thus, in the macrocycle with zero, two and four nitrogens the Pb^{2+} ion exists in the "inactive" form while in the all–nitrogen donor macrocycle, the Pb^{2+} ion is "active". Similar behaviour is reported (110) for 12– and 15–membered mixed–donor macrocycles containing nitrogen and oxygen donors.

The difference between the 18–ane N_4O_2 macrocycle shown in Fig. 3.2.4 and that reported in this work, is the relative positions of the N–donors. The former is trans–18–ane N_4O_2 and the latter cis–18–ane N_4O_2. Both the macrocycles show similar complex stabilities (111). Thus, the lower stability observed for the Pb^{2+} metal ion with the ligand cis–18–ane N_4O_2 is probably due to Pb^{2+} being in the "inactive" form since this form is thought to exist in trans–18–ane N_4O_2. In order to support this theory, the crystal structure of the complex would have had to be determined. Unfortunately, attempts to prepare crystals of the complex [Pb–trans–18–ane N_4O_2][NO_3]$_2$ were unsuccessful.

It is clear from the above discussion that high complex stability for Pb^{2+} can be obtained when Pb^{2+} is in the "active" form. Therefore, when designing ligands it is necessary to predict beforehand whether Pb^{2+} in the complex will be "active" or "inactive".

Since the ligands 15–ane N_3O_2 and 18–ane N_4O_2 did not produce a satisfactory Pb^{2+}/Zn^{2+} selectivity, it was necessary to increase the number of oxygen donors in these macrocycles in such a way as to increase the steric strain in the ligand. Ligands which are sterically more demanding will produce a marked destabilization of the complexes formed with small metal ions relative to those formed with large metal ions. In this way a higher Pb^{2+} over Zn^{2+} selectivity can be achieved. The addition of pendent arms containing oxygen donor groups to these macrocycles will thus serve as a means of introducing steric strain, since macrocycles containing pendent arms are bulkier than unsubstituted macrocycles

3.3 MACROCYLES WITH PENDENT ARMS HAVING OXYGEN DONOR GROUPS

The properties of a macrocycle can be significantly changed when extra potential donors are added to the macrocycle as pendent arms, so that more stable complexes can be formed, or its specificity in metal binding increased. Ligands which have neutral oxygen donor groups as pendent arms have been extensively synthesized, partly because of the synthetic simplicity associated with the reactions. It has been shown (62) that addition of neutral oxygen donors in the form of hydroxyalkyl groups to existing ligands produces metal ion size selectivity patterns very much like those obtained for macrocycles. Thus, in Fig. 3.3.1, the change in Pb^{2+}/Zn^{2+} selectivity is shown when hydroxyalkyl groups are added to EN and 18–ane N_2O_4 to form THPED and DHP–18–ane N_2O_4 respectively.

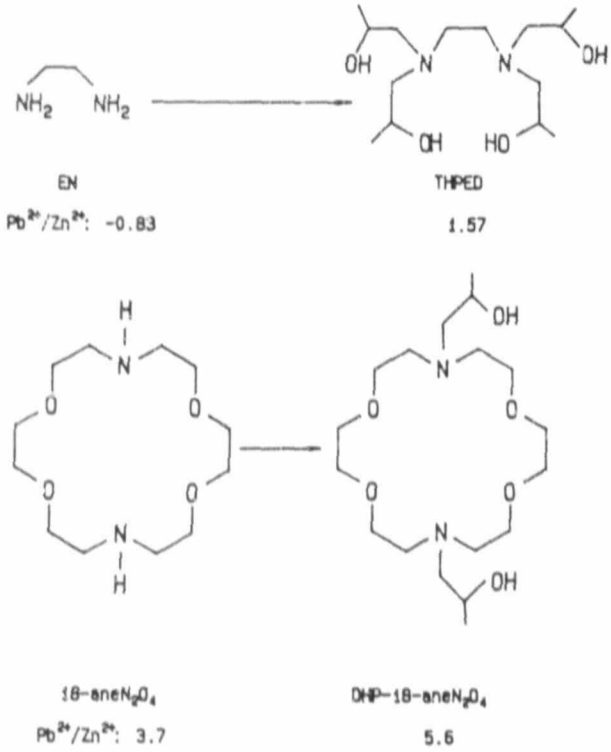

Fig. 3.3.1 Effect of addition of hydroxypropyl groups to existing ligands on the Pb^{2+}/Zn^{2+} selectivity. The Pb^{2+}/Zn^{2+} selectivity is log K_1 (Pb^{2+}) minus log K_1 (Zn^{2+}).

It is clear from Fig. 3.3.1 that Pb^{2+}/Zn^{2+} selectivity can be greatly improved by the addition of oxygen donor bearing groups. The size–selectivity displayed by these ligands has been discussed mainly in terms of the balance between steric and inductive effects (62). For small metal ions steric effects outweigh the favourable inductive effects and a nett decrease in complex stability occurs. Therefore, the selectivity of large metal ions over small metal ions can be sharply increased by employing sterically more demanding ligands. This can be achieved through the use of pendent arms. The addition of pendent arms is synthetically much simpler than creating a cryptand type of structure.

We thus consider here a series of ligands where the addition of an increasing number of oxygen donors in a progressively more sterically demanding fashion is aimed at greatly increasing selectivities for large metal ions such as Pb^{2+} over small metal ions such as Zn^{2+}. The structures of these ligands are shown in Fig. 3.3.2. The formation constants for these ligands with a variety of metal ions are given in Table 8 together with some literature values for comparison purposes.

In Fig. 3.3.3 is shown the relation of Δ log K versus ionic radius for the changes in complex stability accompanying the addition of two ethereal oxygens and three hydroxypropyl groups to DIEN to give THP–15–aneN_3O_2. There is a linear dependence of Δ log K on ionic radius, indicating that the change in complex stability is size related i.e. larger metal ions prefer the addition of oxygen donors while smaller metal ions show a decrease in complex stability when oxygen donors are added to existing ligands. The decrease in complex stability associated with complexes formed by small metal ions is due to steric strain produced by the three pendent arms. The relationship in Fig. 3.3.3 re–emphasizes the fact that addition of neutral oxygen donors increases selectivity for large metal ions over small metal ions. Thus, a Pb^{2+}/Zn^{2+} selectivity of 1.8 log units is found in THP–15–aneN_3O_2

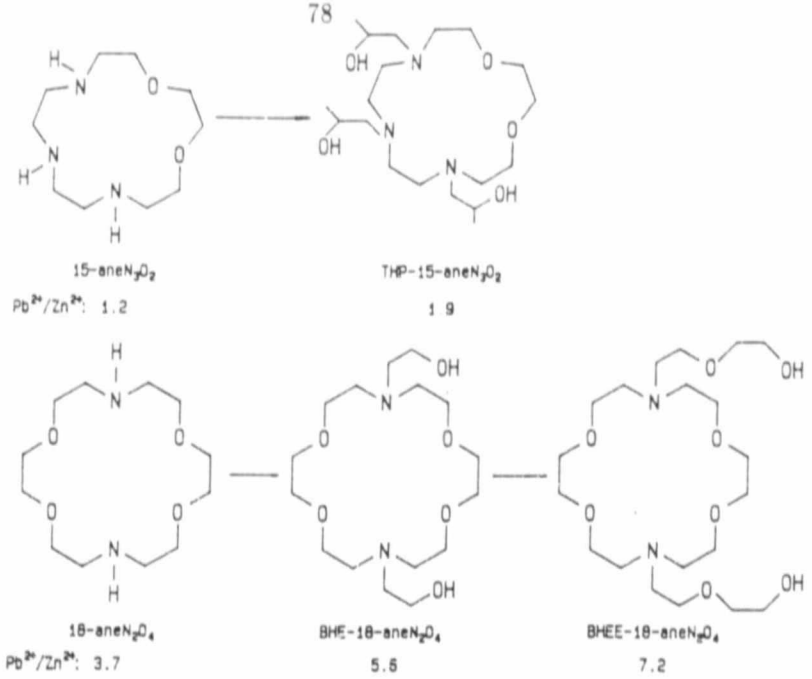

Fig. 3.3.2 Structures of some ligands discussed in this work, and their selectivity of Pb^{2+} over Zn^{2+}. The selectivity, Pb^{2+}/Zn^{2+} indicated, is simply log K_i for the Pb^{2+} complex minus log K_i for the Zn^{2+} complex.

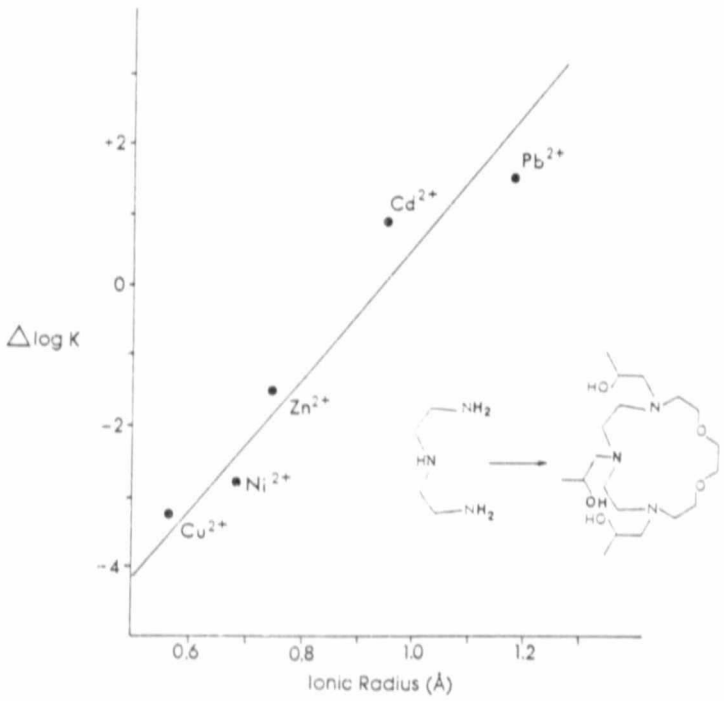

Fig. 3.3.3 The change in complex stability Δ log K, as a function of metal ion radius, in going from DIEN to THP–15–ane N_3O_2. Ionic radii taken from Ref. 98.

Table 8 The formation constants (Log K_1) of a variety of metal ions with the ligands studied in this work together with those of some structurally similar ligands for comparison

	Ionic[a] Radii/Å	THP–15–ane N_3O_2[b]	BHE–18–ane N_2O_4[c]	BHEE–18–ane–N_2O_4[b]
pKa_1		8.8 (1)		8.03(1)
pKa_2		6.70(1)		6.92(1)
pKa_3		1.93(1)		
Ni^{2+}	0.70	7.78(1)		NEC[d]
Cu^{2+}	0.62	12.68(2)	6.6	NEC
Zn^{2+}	0.75	7.21(1)	(3.6)	NEC
Cd^{2+}	0.95	9.15(2)	8.0	3.30(5)
Ca^{2+}	1.00		4.1	NEC
Sr^{2+}	1.16			3.27(1)
Pb^{2+}	1.18	9.09(2)	9.2	7.21(2)
Ba^{2+}	1.36		(5.3)	4.91(1)
Pb^{2+}/Zn^{2+}		1.8	5.6	7.2

a Ref. 98

b This work, 25°C, 0.1M $NaNO_3$

c Ref. 132

d NEC = No evidence of complex formation

Pb^{2+}/Zn^{2+} for each ligand is the log K_1 (Pb^{2+}) min log K_1 (Zn^{2+})

compared to –1.2 in DIEN. The selectivity of 1.8 log units is not much higher than 1.44 log units of EDTA and thus a poor reagent for use as a lead–detoxifying agent. The low Pb^{2+}/Zn^{2+} selectivity in THP–15–ane N_6O_2 suggests that the level of steric crowding is not high enough since the metal ion Zn^{2+} is still able to form a relatively strong complex.

An interesting set of ligands where the addition of an increasing number of oxygen donors leads to progressively more sterically crowded ligands is 18–ane N_2O_4 going to BHE–18–ane N_2O_4 and BHEE–18–ane N_2O_4, shown in Fig. 3.3.2. The selectivities of this series of ligands for the large Pb^{2+} over the small Zn^{2+} are seen in Fig. 3.3.2. It is clear from this figure that as the number of oxygen donor atoms is increased, so does the Pb^{2+}/Zn^{2+} selectivity. Thus, addition of two hydroxyethyl arms to 18–ane N_2O_4 to form BHE–18–ane N_2O_4 results in a 1.9 log unit increase in the Pb^{2+}/Zn^{2+} selectivity. Addition of a further two oxygen donors to BHE–18–ane N_2O_4 to give BHEE–18–ane N_2O_4 now results in a dramatic 3.5 log unit increase in Pb^{2+}/Zn^{2+} selectivity. This increase in Pb^{2+}/Zn^{2+} selectivity clearly demonstrates that it is not necessarily addition of neutral oxygen donors so as to form a macrocyclic ring that produces the most dramatic increase in Pb^{2+}/Zn^{2+} selectivity. Rather, what appears to be important is that a sufficient number of oxygen donor atoms should be added so that a critical level of steric crowding around the metal ion is achieved. The large Pb^{2+}/Zn^{2+} selectivity observed in BHEE–18–ane N_2O_4 can be interpreted in terms of steric crowding. In the case of BHE–18–ane N_2O_4 the steric crowding appears to be moderate and the smaller metal ion Zn^{2+} is capable of adapting to the level of steric crowding required. With the progressive increase in steric crowding, as with the formation of BHEE–18–ane N_2O_4 from BHE–18–ane N_2O_4, the Zn^{2+} is no longer able to accommodate the level of steric crowding required and thus no complex formation occurs. The larger Pb^{2+} ion is still able to adapt to the high level of steric crowding and thus a large increase in Pb^{2+}/Zn^{2+} selectivity occurs.

The observed selectivities can be analyzed more closely on a quantitative basis. As noted above, the change in complex stability produced on adding groups containing neutral oxygen donors appears to be governed by metal ion size. The change in complex stability, Δ log K, is so closely related to metal ion size that a reasonable linear correlation of Δ log K vs ionic radii of the metal ion can be obtained. However, in Fig. 3.3.4 it is seen that when two hydroxyethyl groups are added to 18–ane N_2O_4 to give BHE–18–ane N_2O_4, "plateau" behaviour results, indicating very little dependence of Δ log K on ionic radius for metal ions with an ionic radius greater than about 0.9Å. The same type of "plateau" behaviour has been observed in crown ethers (25,29).

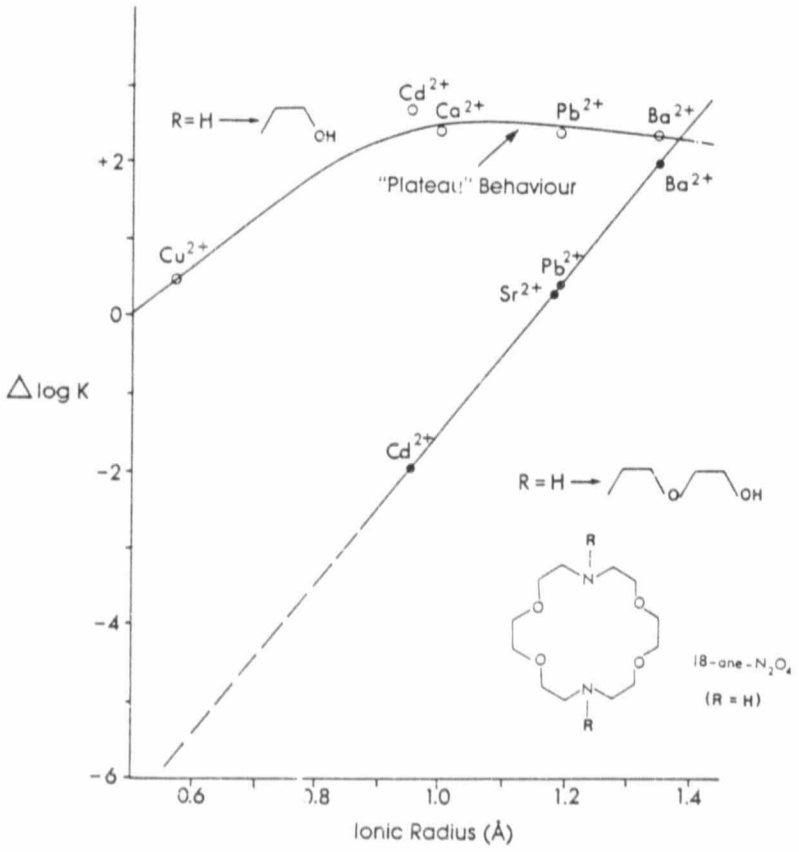

Fig. 3.3.4 The change in complex stability, Δ log K, as a function of metal ion radius as CH_2CH_2OH groups are added to 18–ane N_2O_4 to form BHE–18–ane N_2O_4 (o) and when $CH_2CH_2OCH_2CH_2OH$ groups are added to 18–ane N_2O_4 to form BHEE–18–ane N_2O_4 (•). Ionic radii taken from Ref. 98.

The "plateau" behaviour is interpreted (38) in terms of the balance between steric and inductive effects being constant in the "plateau" region i.e these effects are constant above a certain metal ion size. The "plateau" behaviour results when the added oxygen–donor containing groups lead to a modest increase in steric crowding, typically to ligands which are already of high denticity. However, when the level of steric crowding is further increased by changing the hydroxyethyl groups to hydroxyethyloxyethyl groups, then the changes in complex stability show a strong dependence on metal ion size. Thus, from Table 8, it can be seen that the very large Ba^{2+} metal ion shows only a small decrease in complex stability in going from BHE–18–ane N_2O_4 to BHEE–18–ane N_2O_4. The metal ions Pb^{2+} and Sr^{2+} which are smaller than Ba^{2+} show larger decreases in complex stability for their BHEE–18–ane N_2O_4 complexes relative to BHE–18–ane N_2O_4 complexes, while the medium sized Cd^{2+} ion shows a very large drop in complex stability. The small metal ions such as Cu^{2+} and Zn^{2+} are not complexed at all by BHEE–18–ane N_2O_4. The conclusion is that metal ion size–selectivity can be greatly enhanced when a critical level of steric crowding is achieved. It must be noted that the observed selectivity is associated mainly with ion size and shows no correlation with "hard and soft" acid character, since the large metal ions Ba^{2+}, Pb^{2+} and Cd^{2+} are respectively hard, intermediate, and soft in character.

The above results, as well as those discussed in Section 3.2, where the changes in complex stability accompanying the addition of neutral oxygen donors, have been interpreted mainly in terms of metal ion size. This may appear to be an oversimplification since factors such as coordination geometry and nature of M–L bonding have been ignored. However, if the affinity of the metal ion for oxygen donor ligands is size–related then the difference in complex stability of two metal ions of identical sizes should be constant regardless of the number of oxygen donors but provided that the number of non–oxygen donors remain constant. The comparison of the Pb^{2+} (1.18 Å) over Sr^{2+} (1.17 Å) selectivity should therefore

provide a test of this theory since these metal ions are of almost identical sizes. The Pb^{2+} over Sr^{2+} selectivities are shown in Fig. 3.3.5 for a variety of similar ligands. Particularly interesting is the constant Pb^{2+}/Sr^{2+} selectivity of about 4.2 log units. The constant increase in stability is thus related to the fact that the Pb^{2+} and Sr^{2+} ions are almost identical in size. The constant difference in complexing ability of 4.2 log units reflects the much stronger binding of Pb^{2+} to nitrogen donors than is the case for Sr^{2+}. The Pb^{2+} over Sr^{2+} selectivity changes with change in the number of nitrogen donors. For ligands with a greater number of nitrogen donors the selectivity of Pb^{2+} over Sr^{2+} becomes even larger, so that for the ligand THP–12–ane N_3O, which has three nitrogen donors, the Pb^{2+} over Sr^{2+} selectivity of 8.3 log units is observed (102).

Although there was no evidence of complex formation of Zn^{2+} with BHEE–18–ane N_2O_4, extrapolation of the relation of Δ log K versus ionic radius for the pair of ligands 18–ane N_2O_4 and BHEE–18–ane N_2O_4 in Fig. 3.3.4 suggests that the Pb^{2+}/Zn^{2+} selectivity of BHEE–18–ane N_2O_4 may be approximately 10 log units, which is considerably higher than that of EDTA and a log unit higher than cryptand–2,2,2. Thus, the ligand design approach has yielded promising results since BHEE–18–ane N_2O_4 can be used as a satisfactory reagent as a lead–detoxifying agent. The only drawback the ligand may appear to have is the low complexing strength with Pb^{2+}, since log K_1 is only 7.2 in comparison with the target of 12.0 based on the effectiveness of cryptand–2,2,2. However, in synthetic terms it may be easier to synthesize BHEE–18–ane N_2O_4 than cryptand–2,2,2.

It is clear that by the addition of sufficient neutral oxygen donor atoms the Pb^{2+}/Zn^{2+} selectivity can be increased to high levels. The ligand BHEE–18–ane N_2O_4 does display a satisfactory Pb^{2+}/Zn^{2+} selectivity but there is still a need for improvement of the binding strength of Pb^{2+}. Therefore, the ligand BHEE–18–ane N_2O_4 has to be modified. One way of achieving the high complexing

Author Bhavan Rekha
Name of thesis Ligand Design Using The Neutral Oxygen Donor To Control Metal Ion Size Selectivity. 1989

PUBLISHER:

University of the Witwatersrand, Johannesburg
©2013

LEGAL NOTICES:

Copyright Notice: All materials on the University of the Witwatersrand, Johannesburg Library website are protected by South African copyright law and may not be distributed, transmitted, displayed, or otherwise published in any format, without the prior written permission of the copyright owner.

Disclaimer and Terms of Use: Provided that you maintain all copyright and other notices contained therein, you may download material (one machine readable copy and one print copy per page) for your personal and/or educational non-commercial use only.

The University of the Witwatersrand, Johannesburg, is not responsible for any errors or omissions and excludes any and all liability for any errors in or omissions from the information on the Library website.